Electronic Supplementary Material (ESI) for Dalton Transactions.

Electronic Supporting Information

N,N-Dialkylbenzimidazol-2-ylidene platinum complexes – effects of alkyl residues and ancillary *cis*-ligands on their anticancer activity

Tobias Rehm,[a] Matthias Rothemund,[a] Alexander Bär,[a] Thomas Dietel,[b] Rhett Kempe,[b] Hana Kostrhunova,[c] Viktor Brabec,[c] Jana Kasparkova,*[c] and Rainer Schobert*[a]

[a]*Organic Chemistry Laboratory, University Bayreuth, Universitaetsstrasse 30, 95440 Bayreuth, Germany.*

E-mail: Rainer.Schobert@uni-bayreuth.de

[b] Lehrstuhl fuer Anorganische Chemie II, University Bayreuth, Universitaetsstrasse 30, 95440 Bayreuth, Germany.

[c] Institute of Biophysics, Academy of Sciences of the Czech Republic, CZ-61265 Brno, Czech Republic.

E-mail: jana@ibp.cz

Table of content:

*shared corresponding authors.

General information

All the chemicals and reagents were purchased from Sigma Aldrich, Alfa Aesar, ChemPur or ABCR and were used without further purification. Melting points are uncorrected; NMR spectra were run on a 500 MHz spectrometer; chemical shifts are given in ppm (δ) and referenced relative to the internal solvent signal; ^{195}Pt NMR shifts are quoted relative to Ξ(^{195}Pt) = 21.496784 MHz, K_2PtCl_4 was used as external standard (δ = -1612.81); mass spectra: direct inlet, EI, 70 eV; elemental analyses: Vario EL III elemental analyser; X-Ray Diffractometer: STOE-IPDS II. Synthesis of benzimidazolium salts was performed based on literature procedures[1-3] as described herein.

Synthesis and characterization of benzimidazolium chlorides 6

General procedure:

Benzimidazole (1eq) and the respective alkyl iodides or bromides (5 - 10 eq) in acetonitrile (10 mL/mmol) were treated with K_2CO_3 (1.5 eq) and the mixture was heated to 50 - 70 °C for 1-5 days. After filtration the solvent was evaporated in vacuo and the residue was crystalized from CH_2Cl_2 and hexane.

The resulting benzimidazolium iodides/bromides were then stirred with Ag_2CO_3 (1eq) and conc. HNO_3 (kat.) in Ethanol for 3 h and after filtration of the silver halides the solution was treated with conc. HCl to obtain the respective benzimidazolium chlorides. After neutralization with $NaHCO_3$ and further filtration the solvent was evaporated, and the solids were resuspended in CH_2Cl_2 to filter off all inorganic residues. The product was then crystalized by adding hexane.

Synthesis of 1,3-dimethylbenzimidazolium chloride:[1]

Benzimidazole (472 mg, 4.0 mmol), iodomethane (2.48 mL, 40 mmol, 10 eq) and K_2CO_3 (828 mg, 6.0 mmol, 1.5 eq) in acetonitrile (40 mL) for 5 d at 50 °C gave 1.004 g (92 %) of the benzimidazolium iodide which was treated with Ag_2CO_3 (1.0 g, 3.7 mmol), conc. HNO_3 (100 µL) and conc. HCl (800 µL) in EtOH (80 mL). Yield: 632 mg (87 %) white solid; ^{1}H NMR ($CDCl_3$, 500 MHz): δ 4.21 (6 H, s) 7.67 - 7.71 (2 H, m) 7.71 - 7.76 (2 H, m) 10.75 (1 H, s).

Synthesis of 1,3-diethylbenzimidazolium chloride:[1]

Benzimidazole (500 mg, 4.2 mmol), iodoethane (1.26 mL, 21 mmol, 5 eq) and K_2CO_3 (871 mg, 6.3 mmol, 1.5 eq) in acetonitrile (40 mL) for 24 h at 70 °C gave 1.278 g (100 %) of the benzimidazolium iodide which was treated with Ag_2CO_3 (1.16 g, 4.2 mmol), conc. HNO_3 (100 µL) and conc. HCl (800 µL) in EtOH (80 mL). Yield: 880 mg (100 %) white solid; ^{1}H NMR ($CDCl_3$, 500 MHz): δ 1.77 (6 H, t, *J* = 7.3 Hz) 4.70 (4 H, q, *J* = 7.3 Hz) 7.66 - 7.70 (2 H, m) 7.75 - 7.79 (2 H, m) 11.08 (1 H, s).

Synthesis of 1,3-dibutylbenzimidazolium chloride:[2]

Benzimidazole (2.0 g, 17 mmol), 1-bromobutane (7.2 mL, 68 mmol, 4 eq) and K_2CO_3 (3.5 g, 26 mmol, 1.5 eq) in acetonitrile (150 mL) for 5 d at 70 °C gave 3.635 g (69 %) of the benzimidazolium bromide which was treated with Ag_2CO_3 (3.22 g, 12 mmol), conc. HNO_3 (100 µL) and conc. HCl (800 µL) in EtOH (100 mL). Yield: 2.849 mg (63 %) amber solid; ^{1}H NMR ($CDCl_3$, 500 MHz): δ 0.98 (6 H, t, *J* = 7.5 Hz) 1.44 (4 H, sxt, *J* = 7.5 Hz) 2.02 (4 H, quin, *J* = 7.5 Hz) 4.59 (4 H, t, *J* = 7.5 Hz) 7.64 - 7.68 (2 H, m) 7.70 - 7.74 (2 H, m) 11.46 (1 H, s).

Synthesis of 1,3-dioctylbenzimidazolium chloride:[3]

Benzimidazole (236 mg, 2.0 mmol), 1-bromooctane (1.74 mL, 10 mmol, 5 eq) and K_2CO_3 (414 mg, 3.0 mmol, 1.5 eq) in acetonitrile (20 mL) for 3 d at 70 °C gave 461 mg (54 %) of the benzimidazolium bromide which was treated with Ag_2CO_3 (300 mg, 1.1 mmol), conc. HNO_3 (30 µL) and conc. HCl (200 µL) in EtOH (20 mL). Yield: 398 mg (52 %) white solid; ^{1}H NMR ($CDCl_3$, 500 MHz): δ 0.84 - 0.89 (6 H, m) 1.20 - 1.40 (20 H, m) 2.01 (4 H, quin, *J* = 7.5 Hz) 4.54 (4 H, t, *J* = 7.5 Hz) 7.64 - 7.69 (2 H, m) 7.69 - 7.75 (2 H, m) 11.05 (1 H, s).

Table S 1: X-ray structural data of platinum carbene complexes 8b, 9c and 10a.

Crystal data	**8b**	**9c**	**10a**
Chemical formula	$C_{13}H_{20}Cl_2N_2OPtS$	$C_{33}H_{37}Cl_2N_2PPt$	$C_{45}H_{40}ClN_2P_2Pt{\cdot}Cl$
M_r	518.36	1517.27	936.72
Crystal system, space group	Triclinic, P^{-1}	Triclinic, P^{-1}	Monoclinic, P21/c
Temperature (K)	133	133	133
a, *b*, *c* (Å)	8.675 (5), 9.264 (5), 10.601 (5)	9.1067 (18), 12.792 (3), 13.803 (3)	12.578 (5), 10.790 (5), 32.126 (5)
α, β, γ (°)	91.874 (5), 103.182 (5), 94.722 (5)	88.02 (3), 87.59 (3), 71.06 (3)	90, 94.531 (5), 90
V (Å^3)	825.5 (8)	1519.2 (6)	4346 (3)
Z	2	1	4
F(000)	496	752	1864
D_x (Mg m^{-3})	2085	1.658	1431
Radiation type	Mo *K*α	Mo *K*α	Mo *K*α
No. of reflections for cell measurement	9824	31963	16101
θ range (°) for cell measurement	2.0–28.5	1.5–30.1	1.6–27.7
µ (mm^{-1})	8.95	4.87	3.46
Crystal shape	Needles	Block	Platte
Colour	Colourless	Colourless	Colourless
Crystal size (mm)	0.11 × 0.08 × 0.07	0.36 × 0.19 × 0.15	0.20 × 0.09 × 0.08
Data collection			
Diffractometer	STOE-STADIVARI	STOE-STADIVARI	STOE-STADIVARI
Scan method	ω–scan	ω–scan	ω–scan
Absorption correction	Numerical STOE *X-RED32*	Numerical STOE X-RED32	Numerical SROE X-RED32
T_{min}, T_{max}	0.680, 0.761	0.553, 0.719	0.863, 0.953
No. of measured, independent and observed [$I > 2\sigma(I)$] reflections	7449, 3177, 2704	21191, 5907, 5605	32457, 8450, 5359
R_{int}	0.042	0.022	0.104
θ values (°)	θ_{max} = 26.0, θ_{min} = 2.0	θmax = 26.0, θmin = 1.5	θmax = 26.0, θmin = 1.6
$(\sin\theta/\lambda)_{max}$ (Å^{-1})	0.617	0.617	0.617
Range of *h*, *k*, *l*	*h* = −9 → 10 *k* = −11 → 9 *l* = −13 → 11	h = −5 → 11 k = −15 → 15 l = −16 → 17	h = −15 → 8 k = −13 → 13 l = −39 → 37
Refinement			
Refinement on	F^2	F^2	F^2

$R[F^2 > 2\sigma(F^2)]$, $wR(F^2)$, S	0.033, 0.085, 1.03	0.017, 0.040, 1.04	0.072, 0.190, 0.95
No. of reflections	3177	5907	8450
No. of parameters	185	354	471
No. of restraints	0	0	27
H-atom treatment	H-atom parameters constrained	H-atom parameters constrained	H-atom parameters constrained
Weighting scheme	$w = 1/[\sigma^2(F_o^2) + (0.0485P)^2]$ where $P = (F_o^2 + 2F_c^2)/3$	w = 1/[σ2(Fo2) + (0.0275P)2 + 0.1532P] where P = (Fo2 + 2Fc2)/3	w = 1/[σ2(Fo2) + (0.1181P)2] where P = (Fo2 + 2Fc2)/3
$(\Delta/\sigma)_{max}$	< 0.001	0.001	0.001
$\Delta\rho_{max}$, $\Delta\rho_{min}$ (e Å^{-3})	2.52, −2.72	0.45, −1.24	1.99, −2.96

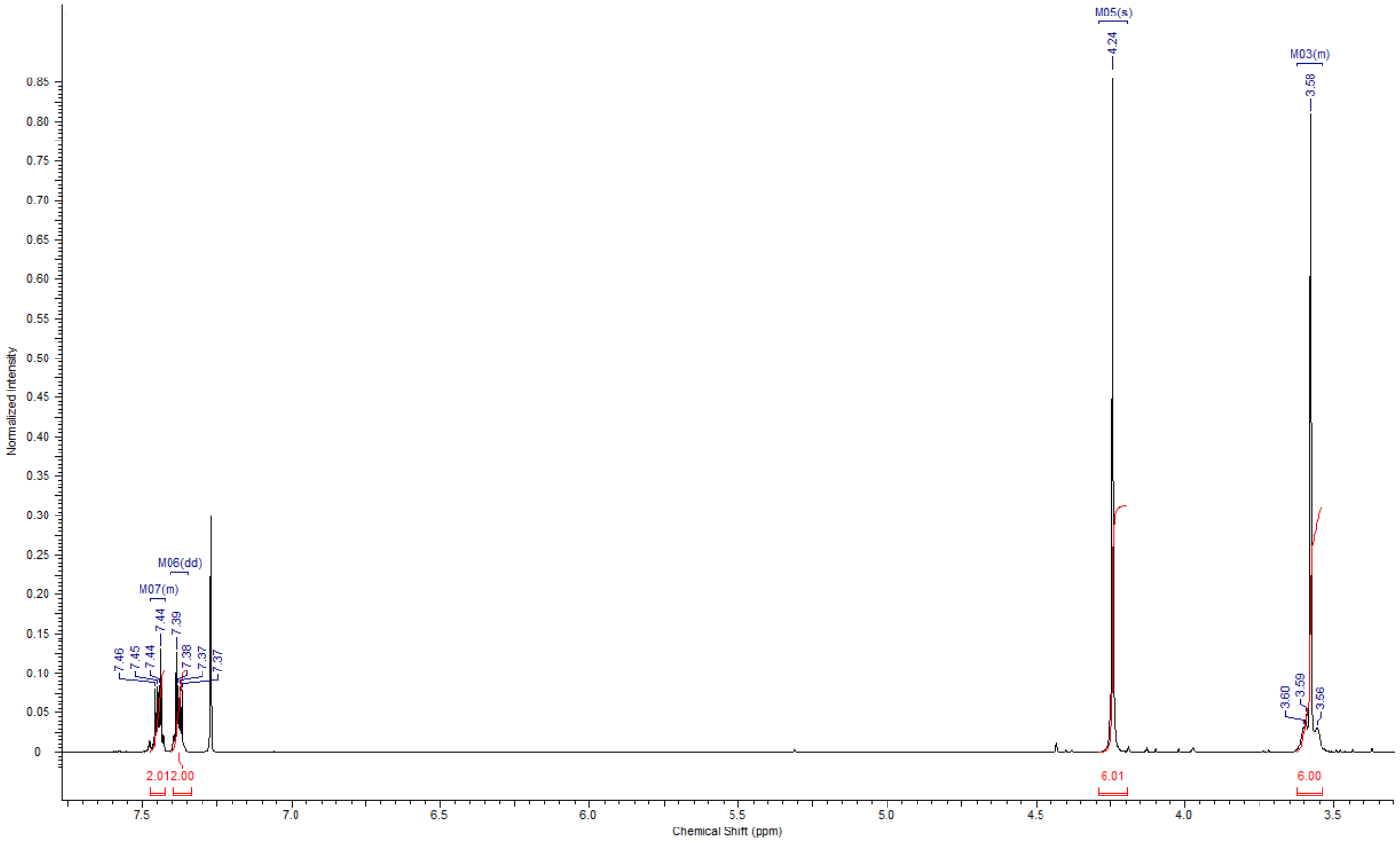

Fig. S1: ^{1}H-NMR spectrum (500 MHz, $CDCl_3$) of complex **8a**.

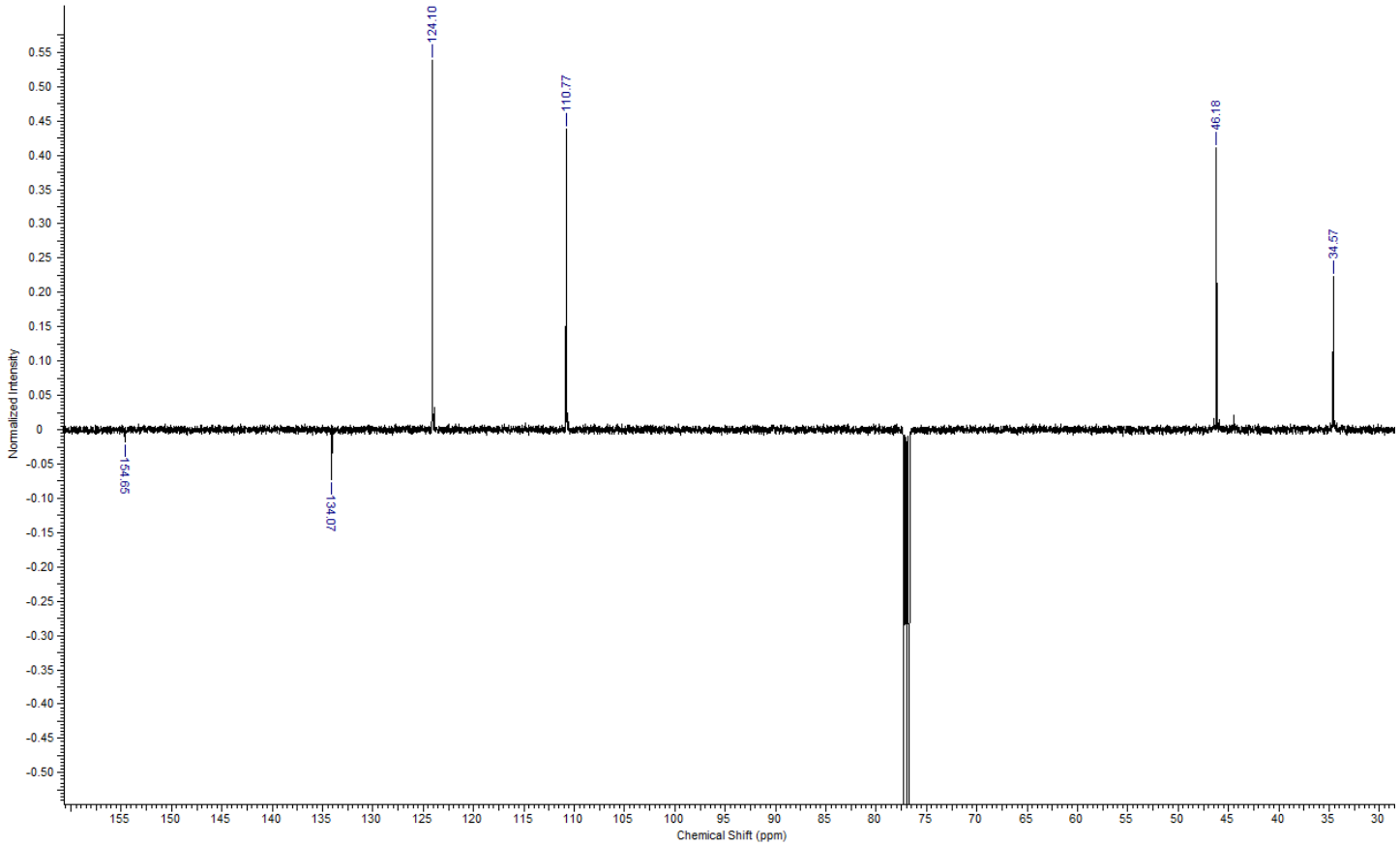

Fig. S 2: ^{13}C-NMR spectrum (126 MHz, $CDCl_3$) of complex **8a**.

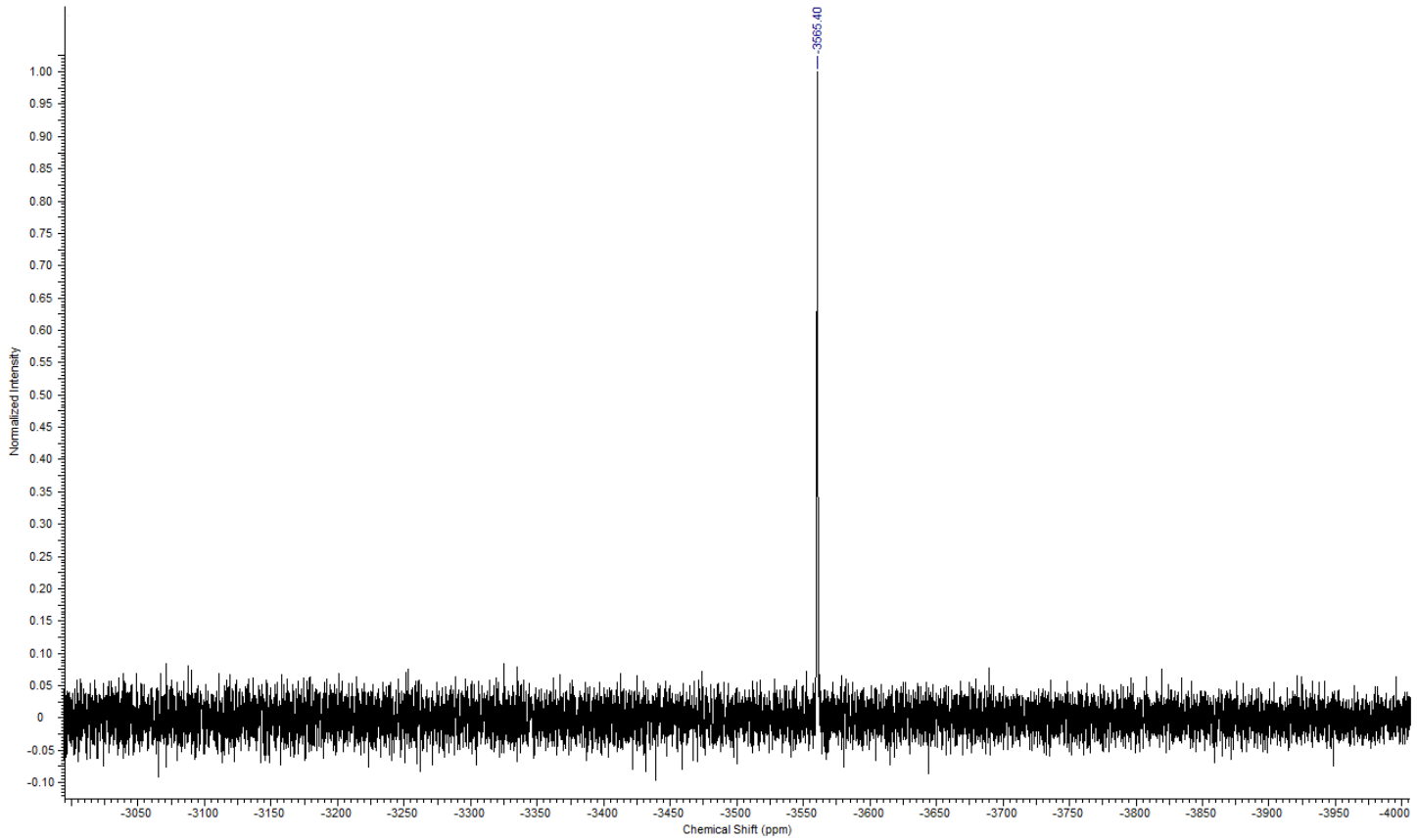

Fig. S 3: ^{195}Pt-NMR spectrum (108 MHz, $CDCl_3$) of complex **8a**.

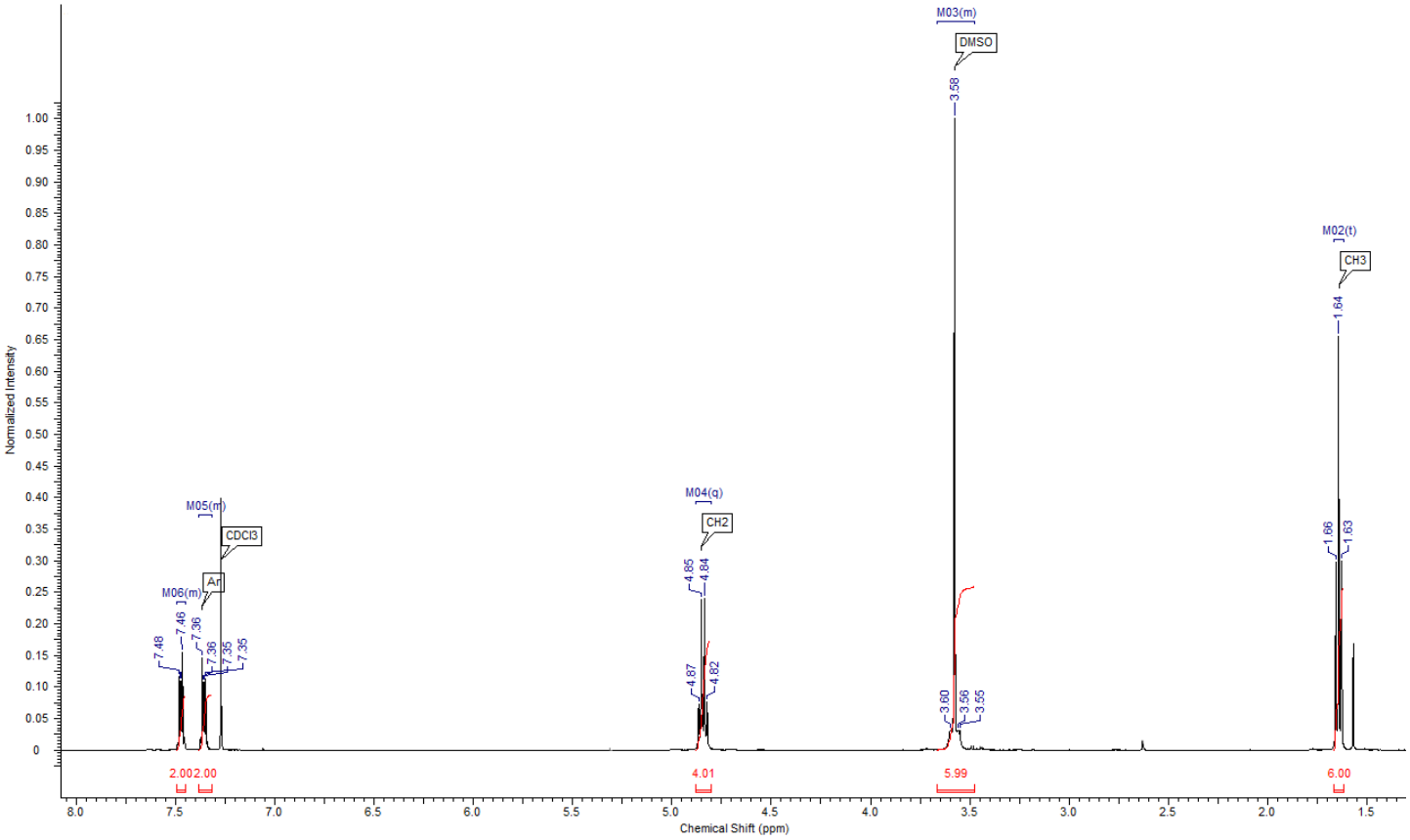

Fig. S 4: ^{1}H-NMR spectrum (500 MHz, $CDCl_3$) of complex **8b**.

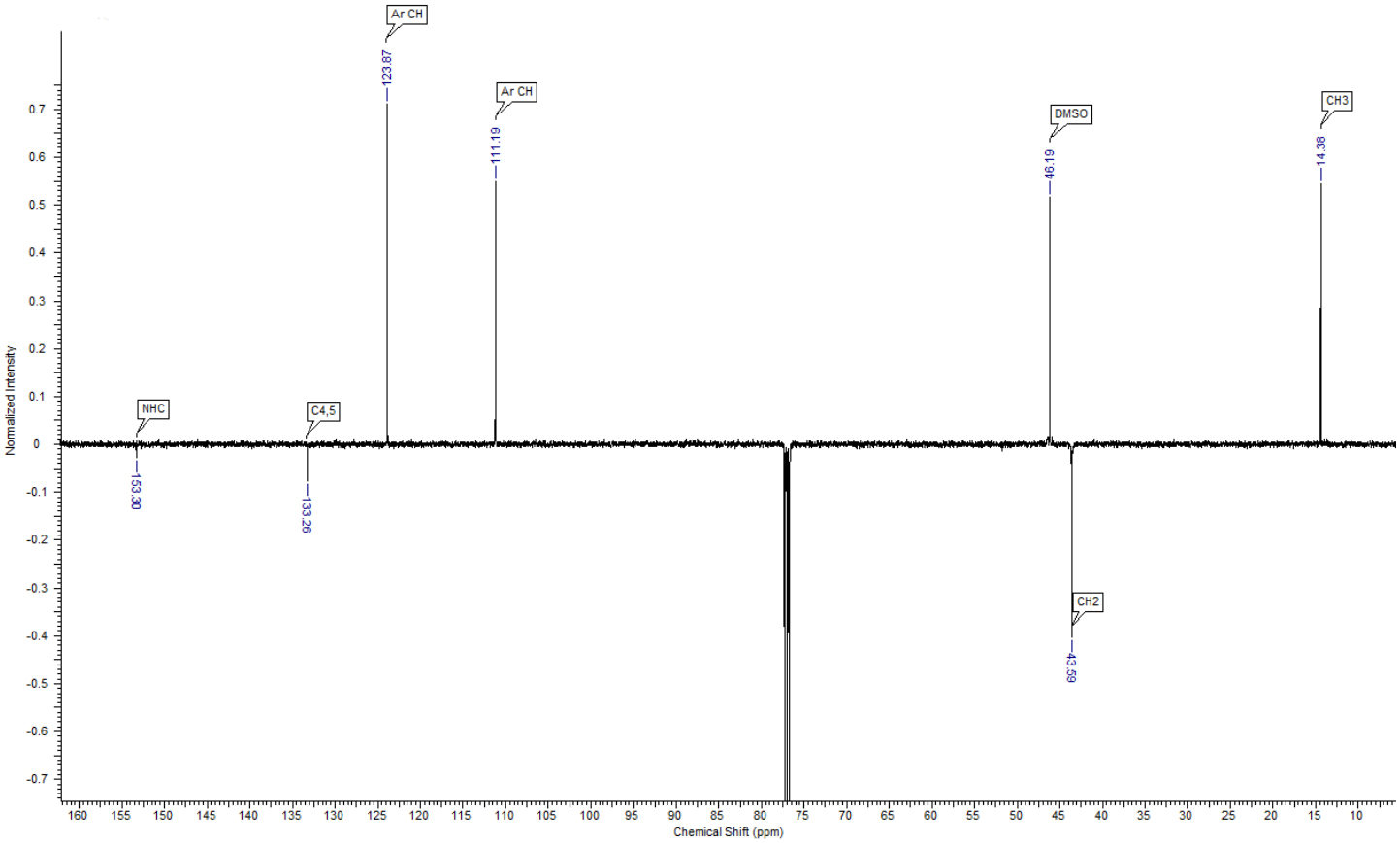

Fig. S 5: ^{13}C-NMR spectrum (126 MHz, $CDCl_3$) of complex **8b**.

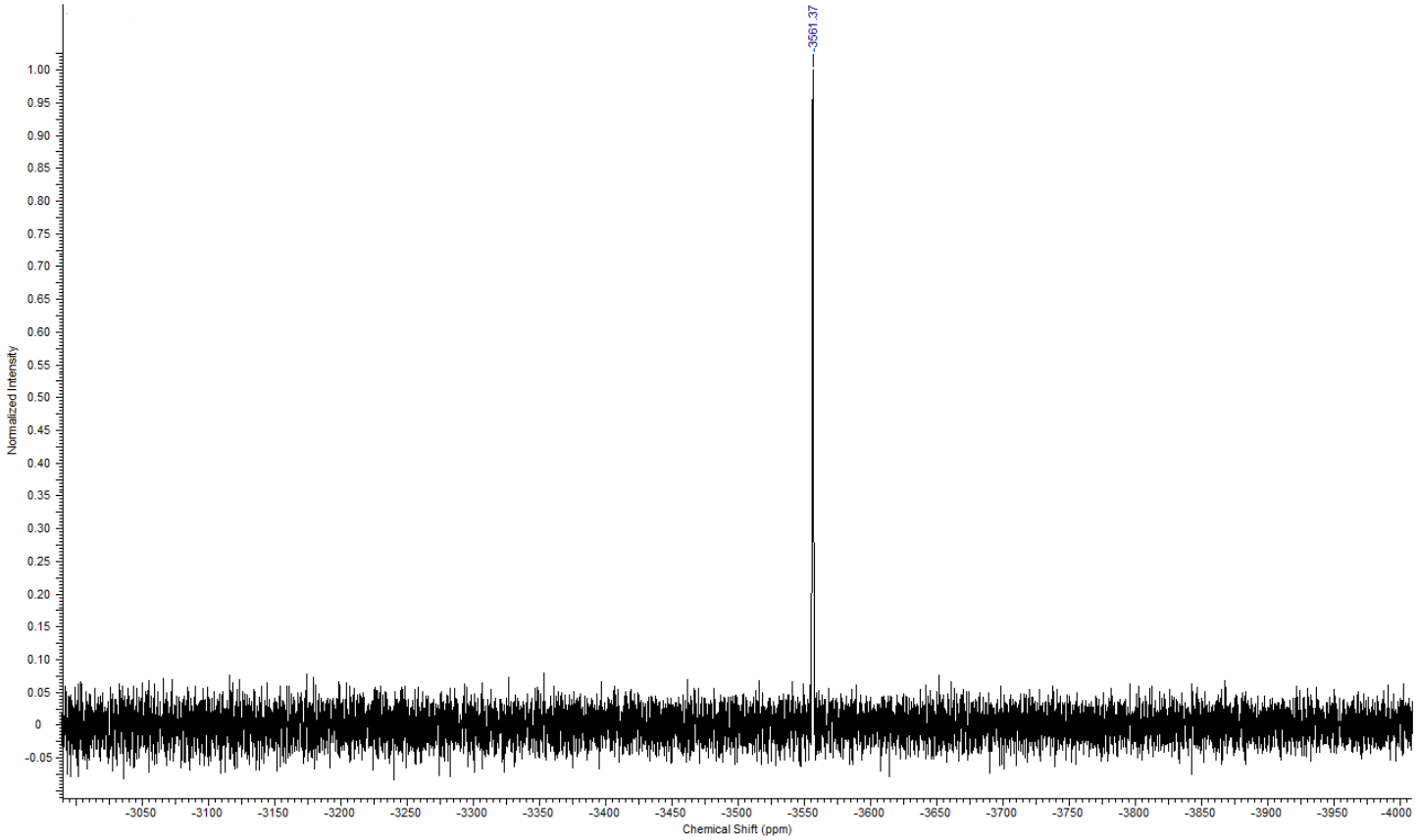

Fig. S 6: ^{195}Pt-NMR spectrum (108 MHz, $CDCl_3$) of complex **8b**.

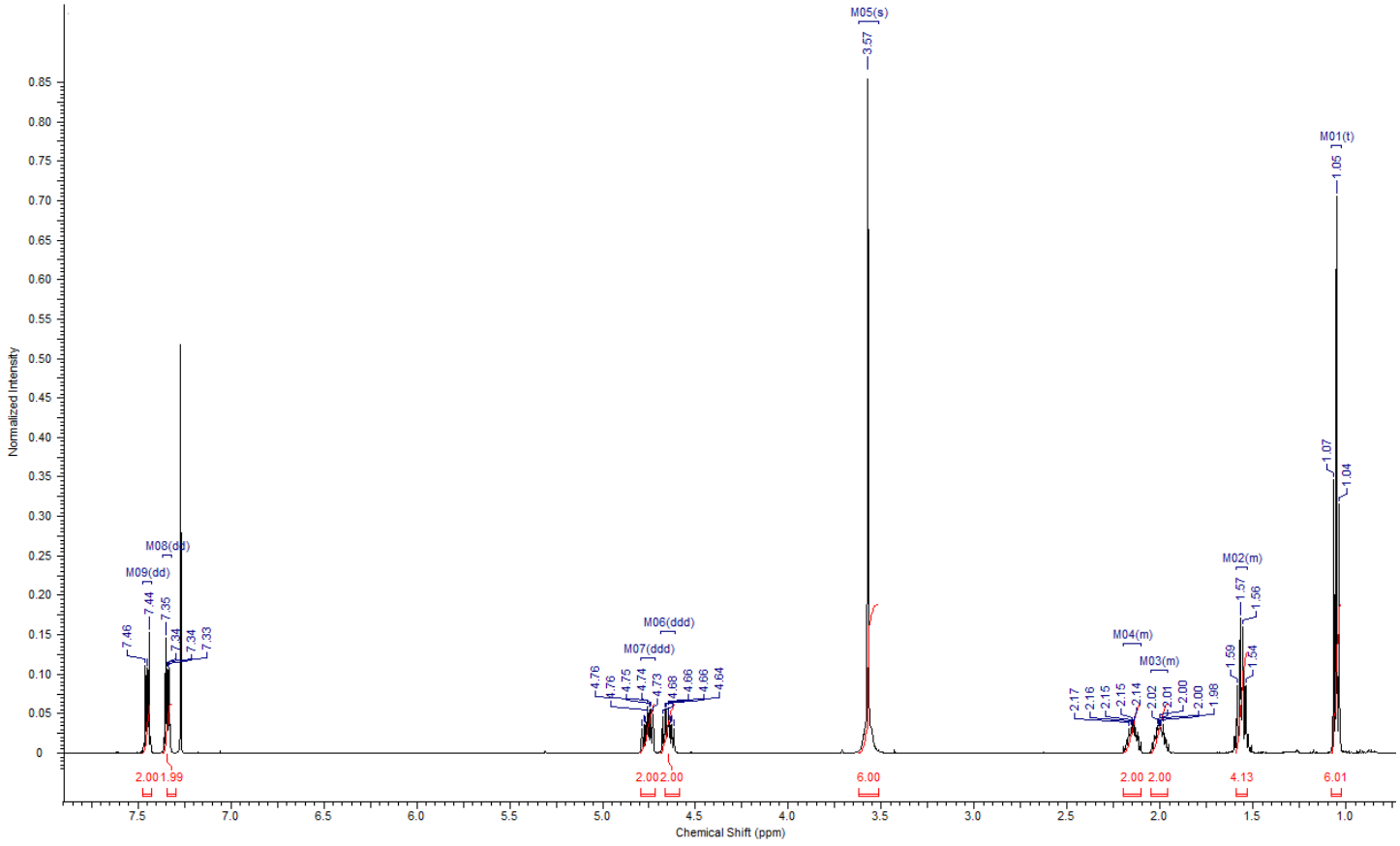

Fig. S 7: ^{1}H-NMR spectrum (500 MHz, $CDCl_3$) of complex **8c**.

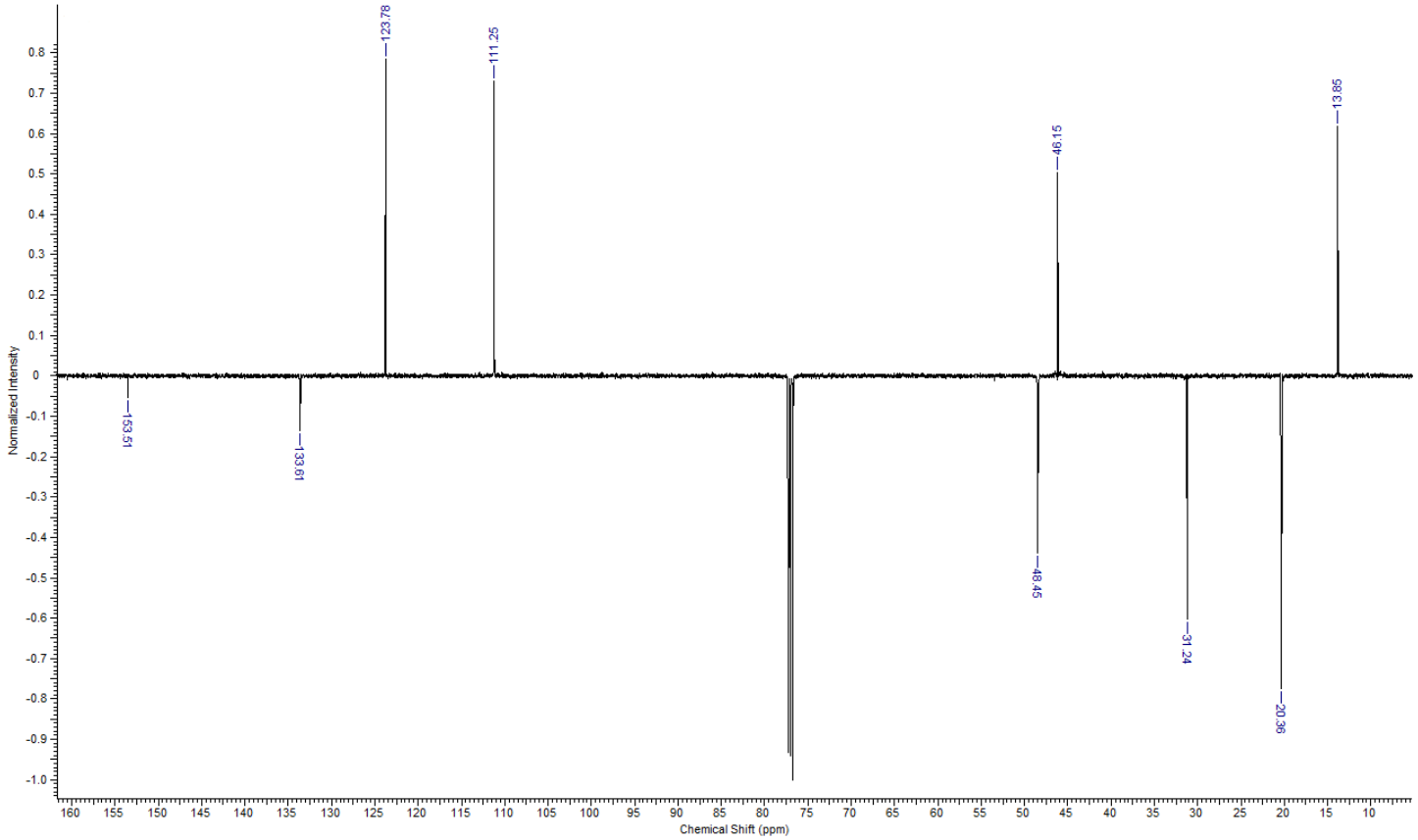

Fig. S 8: ^{13}C-NMR spectrum (126 MHz, $CDCl_3$) of complex **8c**.

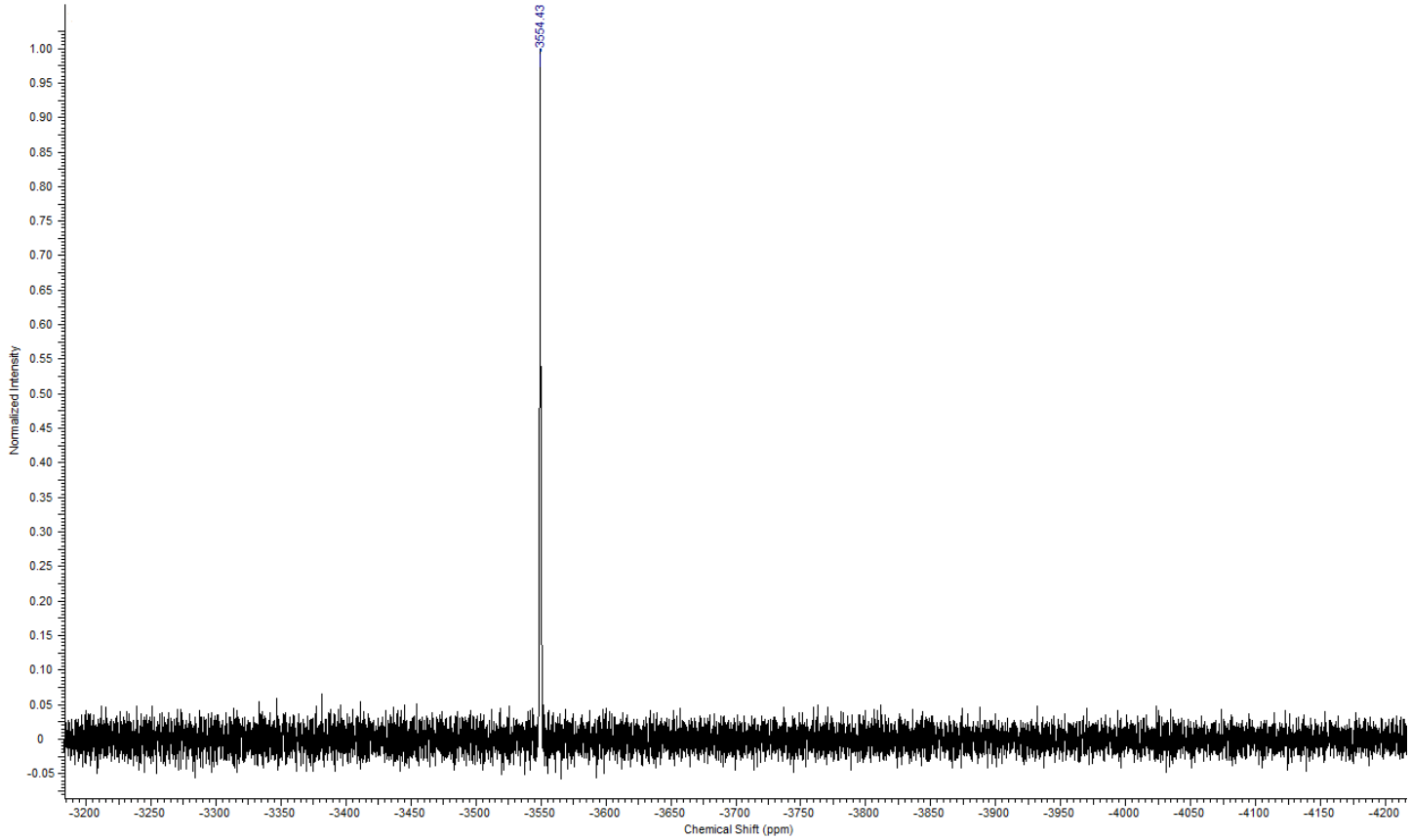

Fig. S 9: ^{195}Pt-NMR spectrum (108 MHz, $CDCl_3$) of complex **8c**.

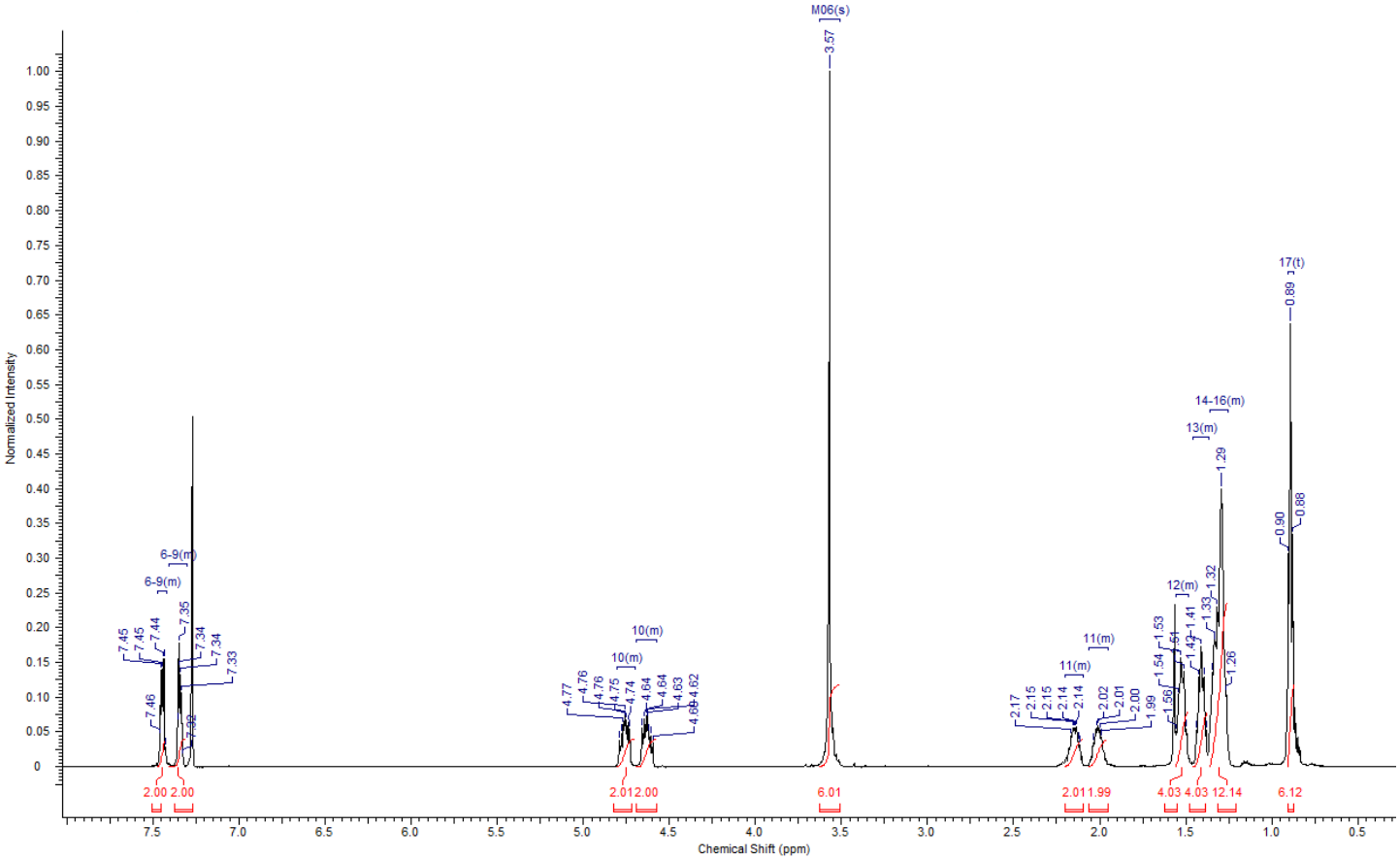

Fig. S 10: ^{1}H-NMR spectrum (500 MHz, $CDCl_3$) of complex **8d**.

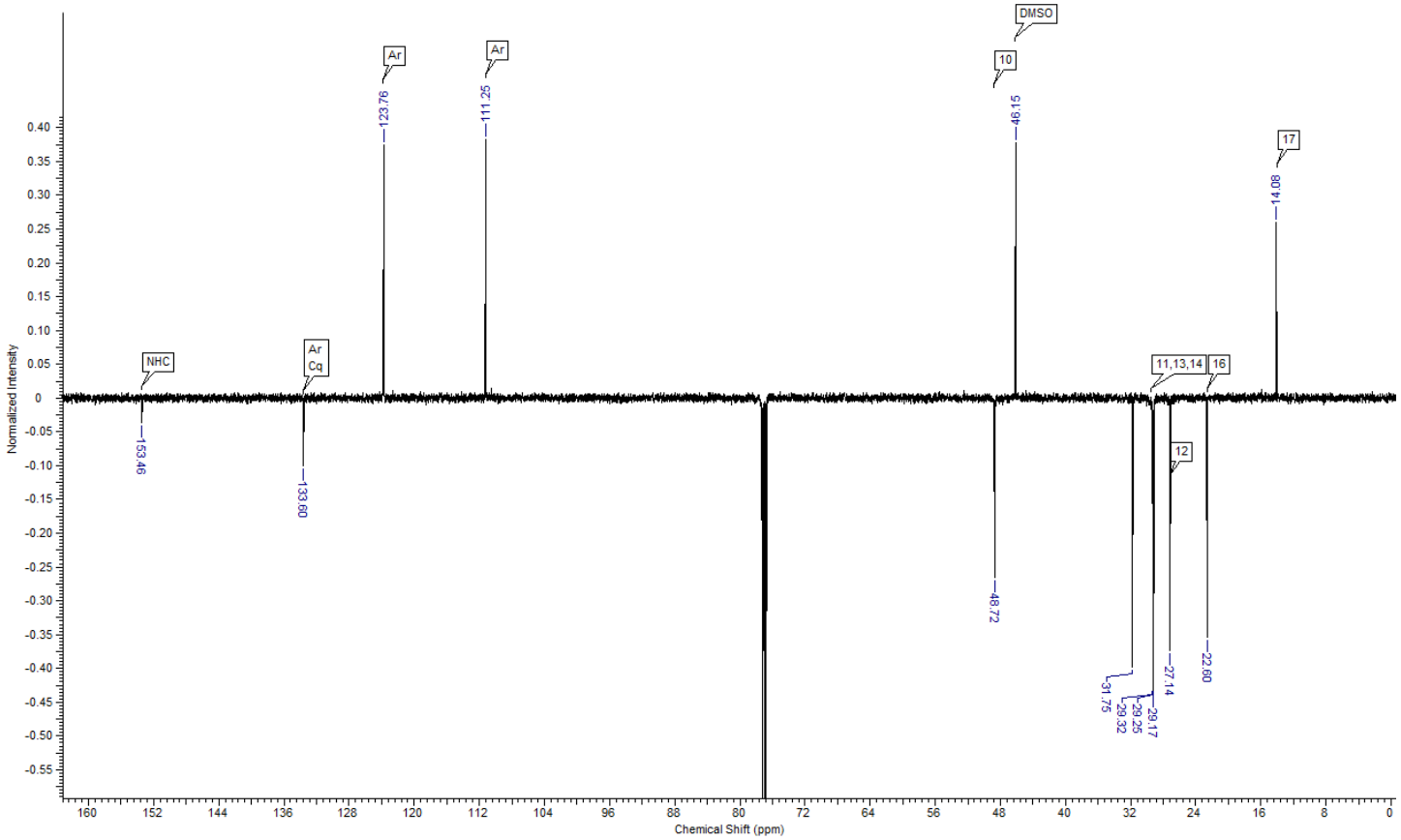

Fig. S 11: ^{13}C-NMR spectrum (126 MHz, $CDCl_3$) of complex **8d**.

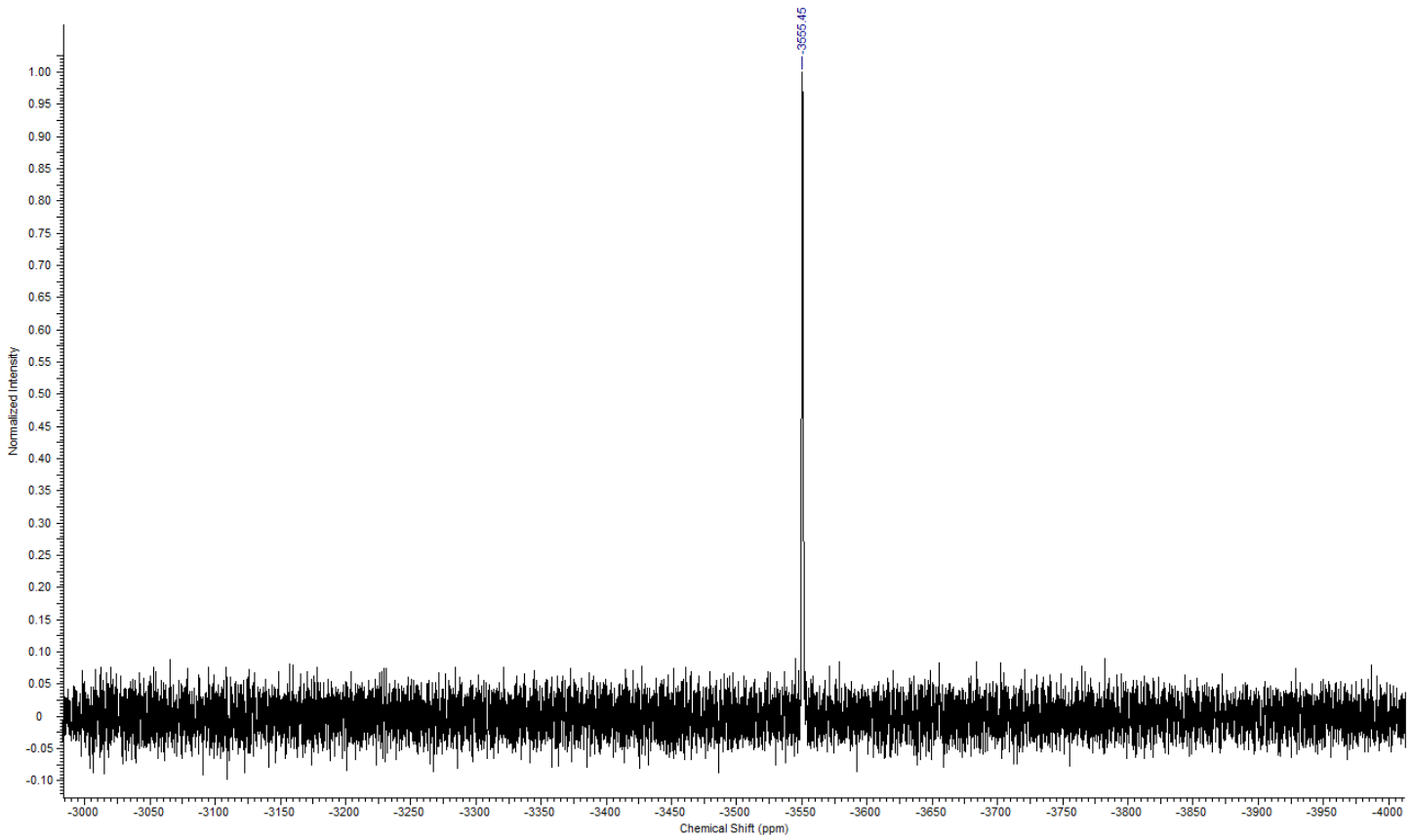

Fig. S 12: ^{195}Pt-NMR spectrum (108 MHz, $CDCl_3$) of complex **8d**.

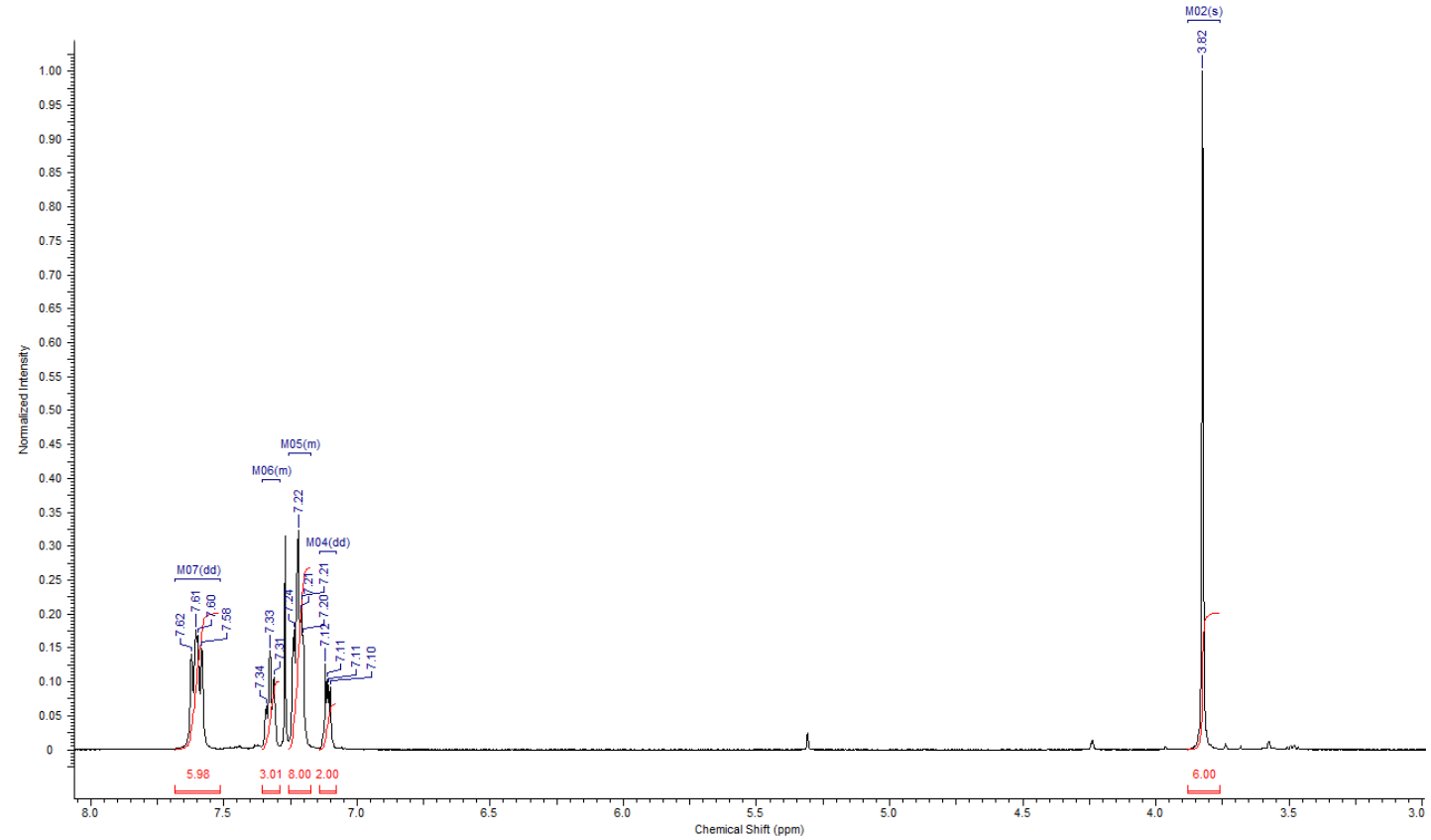

Fig. S 13: ^{1}H-NMR spectrum (500 MHz, $CDCl_3$) of complex **9a**.

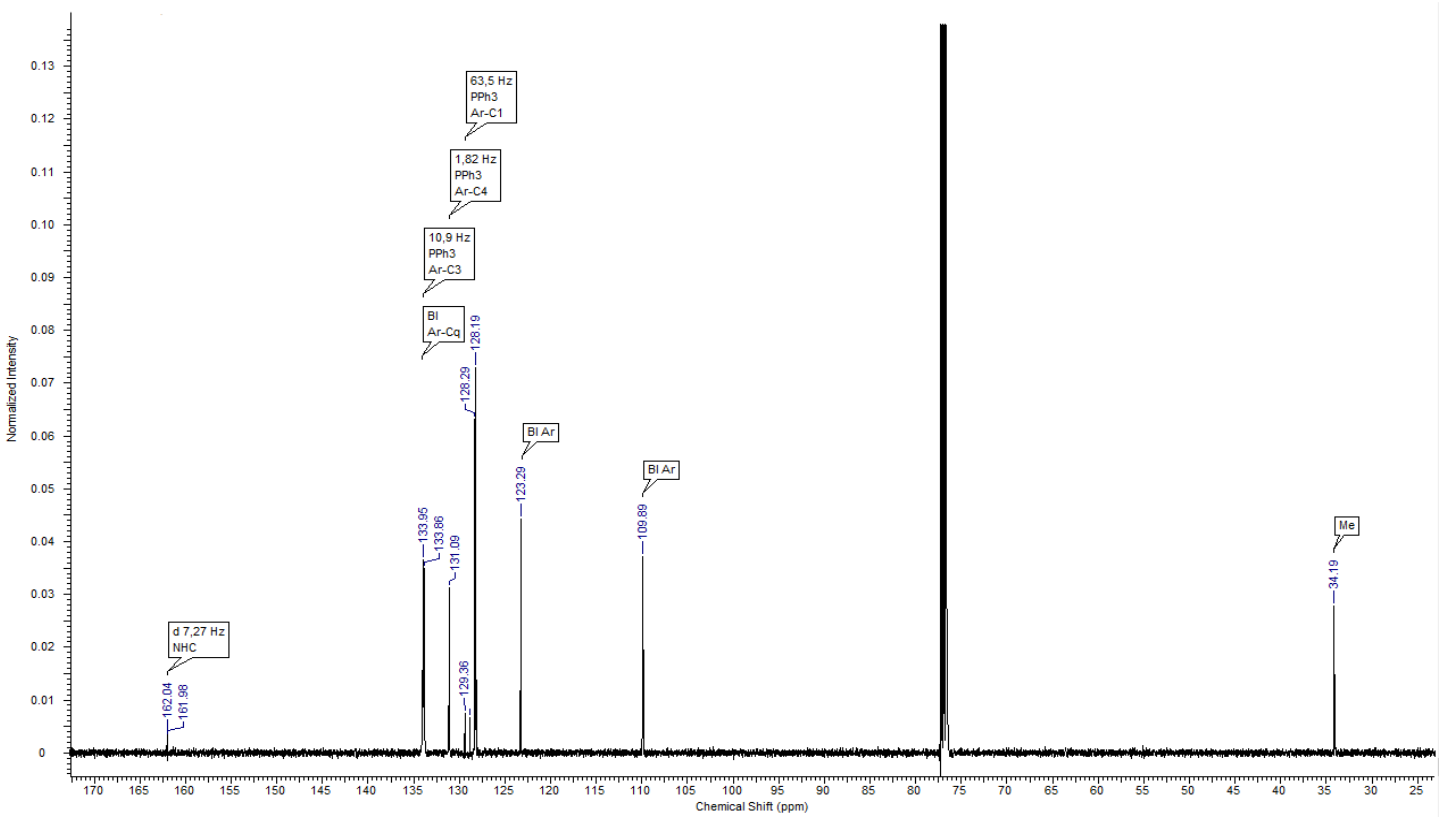

Fig. S 14: ^{13}C-NMR spectrum (126 MHz, $CDCl_3$) of complex **9a**.

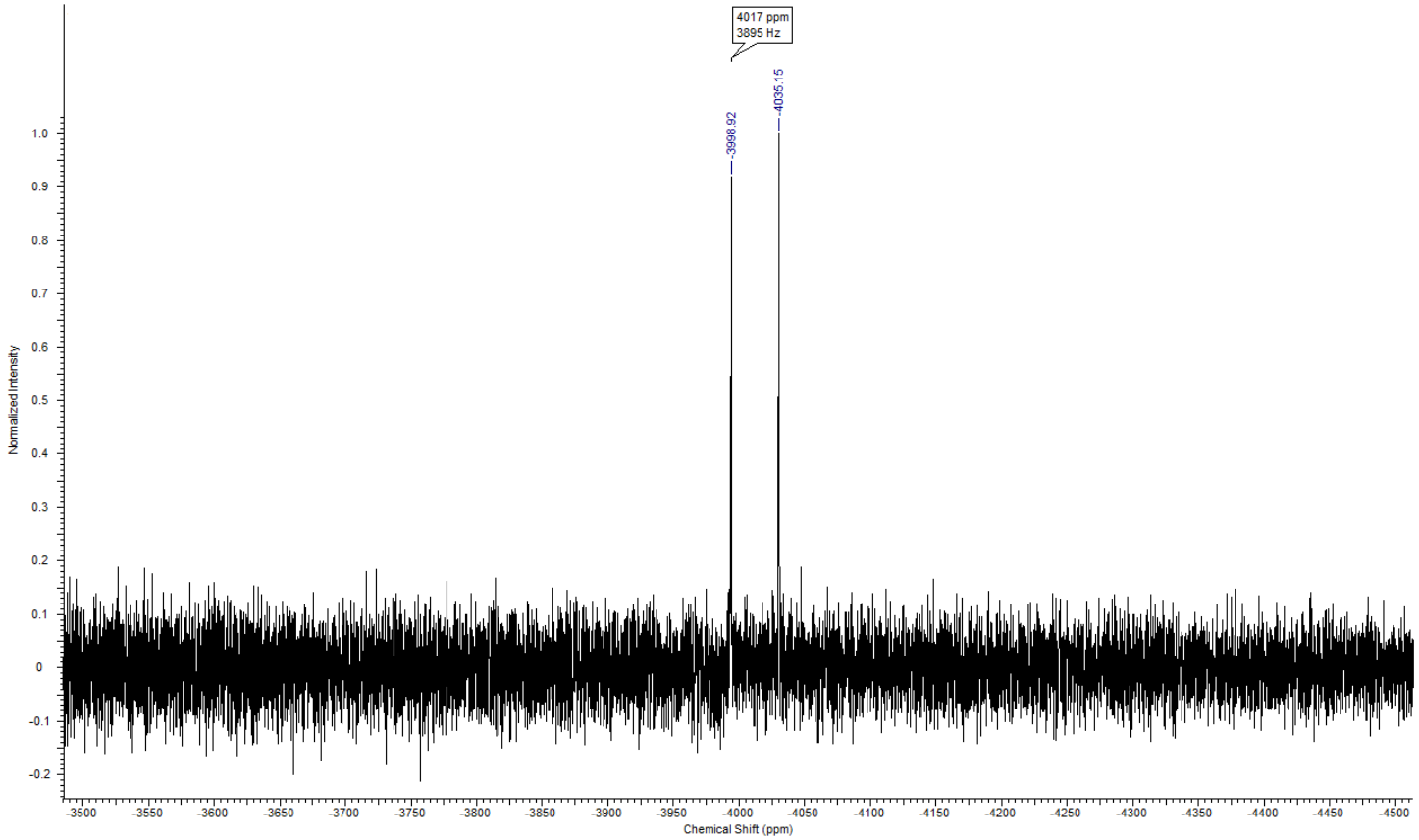

Fig. S 15: ^{195}Pt-NMR spectrum (108 MHz, $CDCl_3$) of complex **9a**.

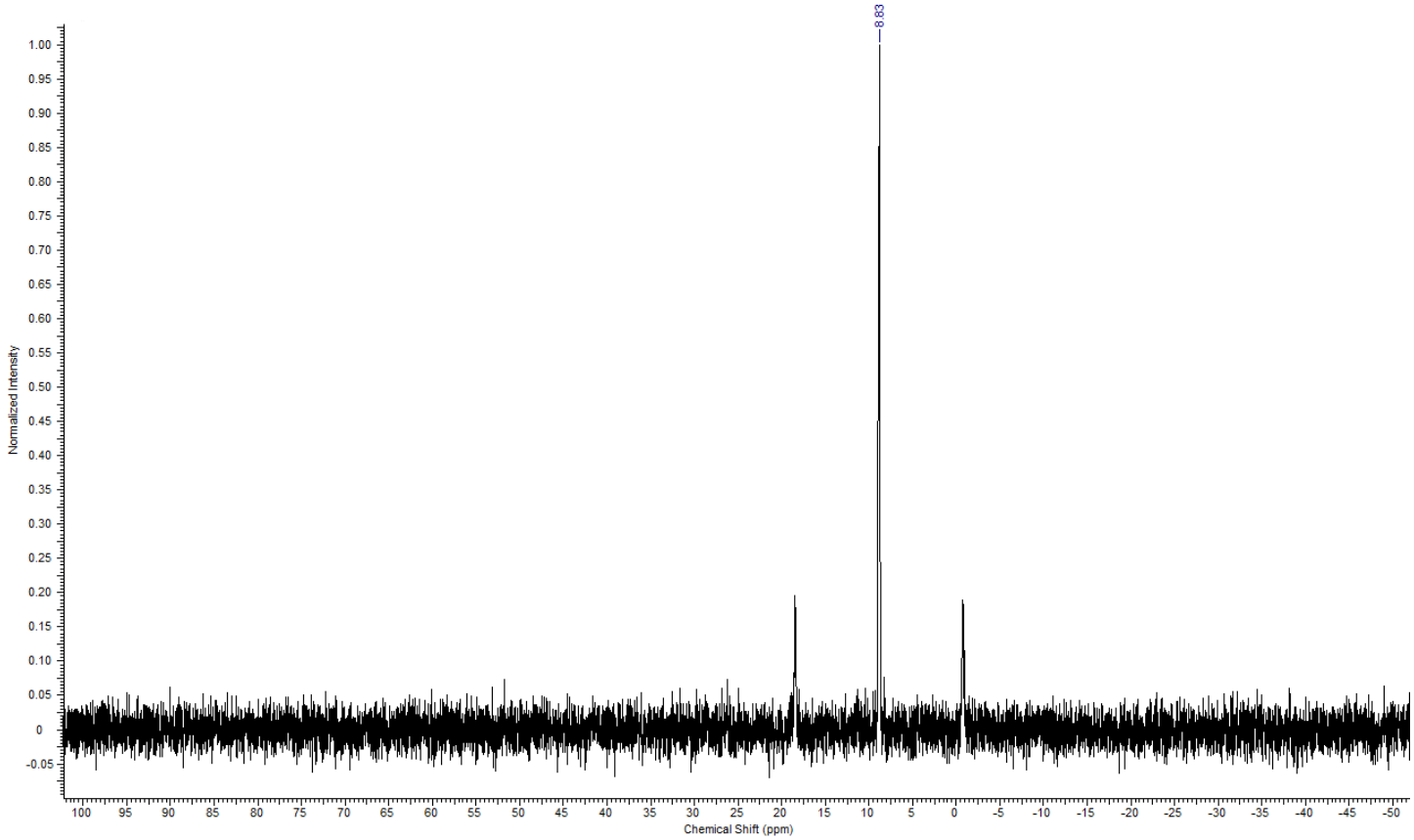

Fig. S 16: ^{31}P-NMR spectrum (202 MHz, $CDCl_3$) of complex **9a**.

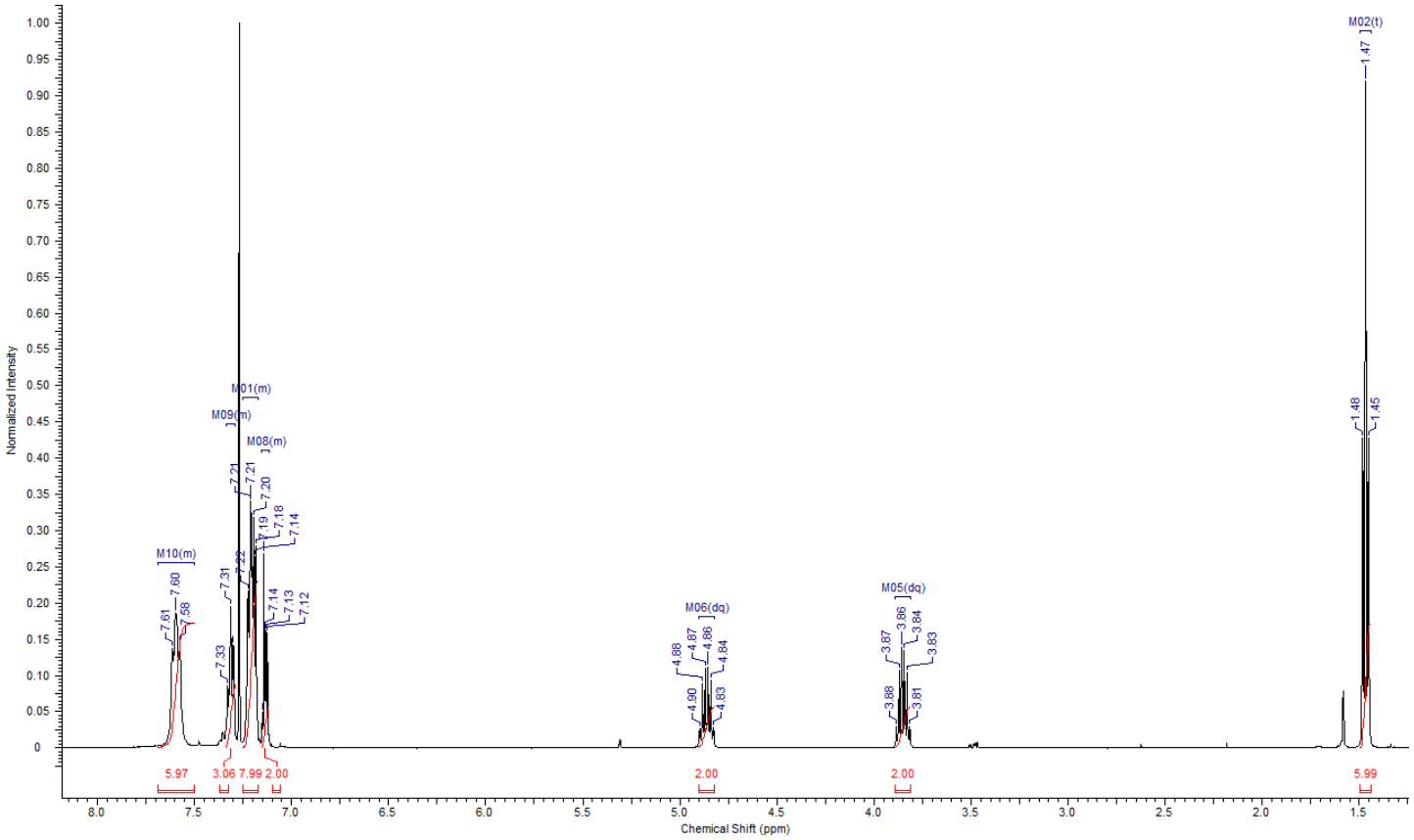

Fig. S 17: ^{1}H-NMR spectrum (500 MHz, $CDCl_3$) of complex **9b**.

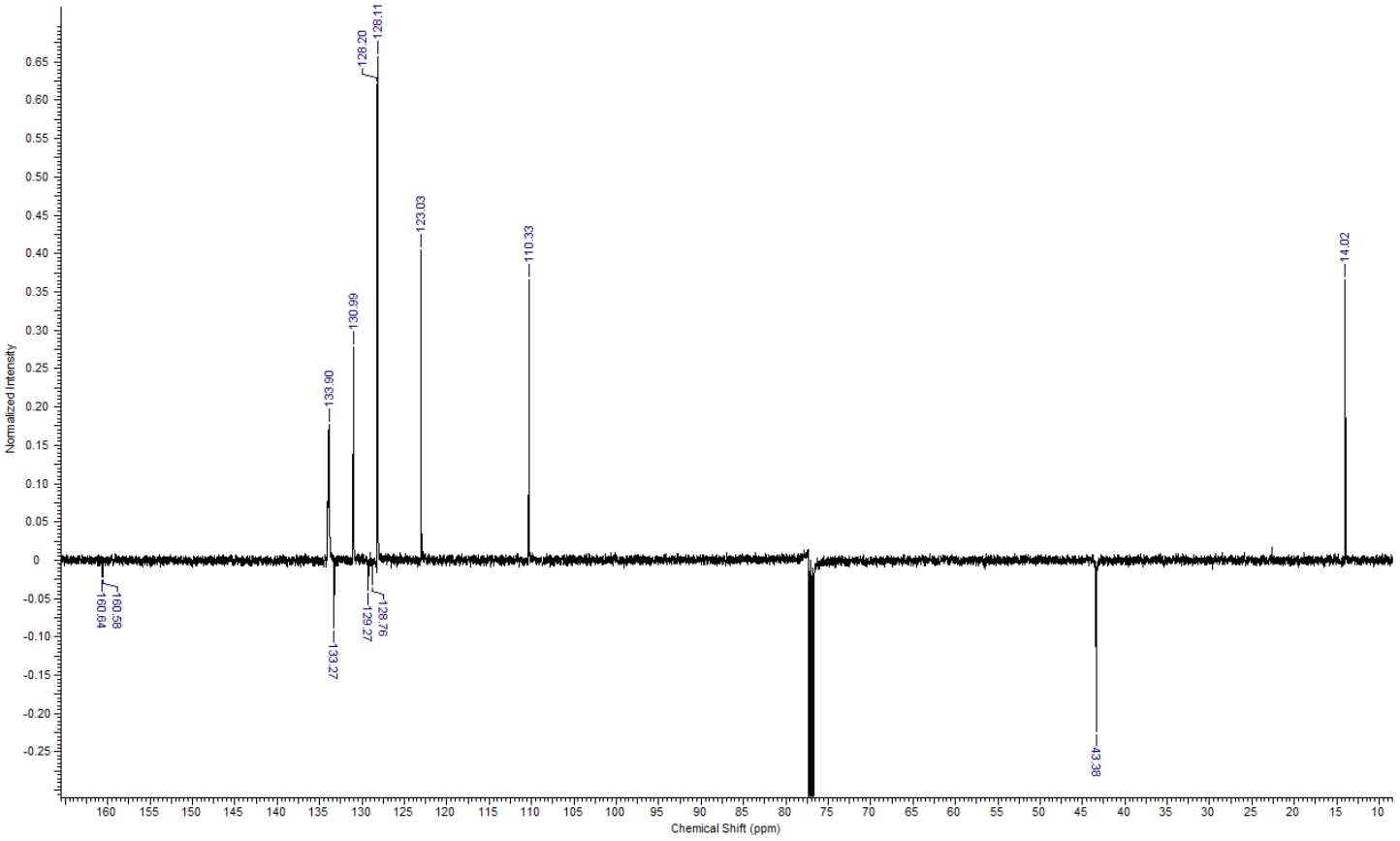

Fig. S 18: ^{13}C-NMR spectrum (126 MHz, $CDCl_3$) of complex **9b**.

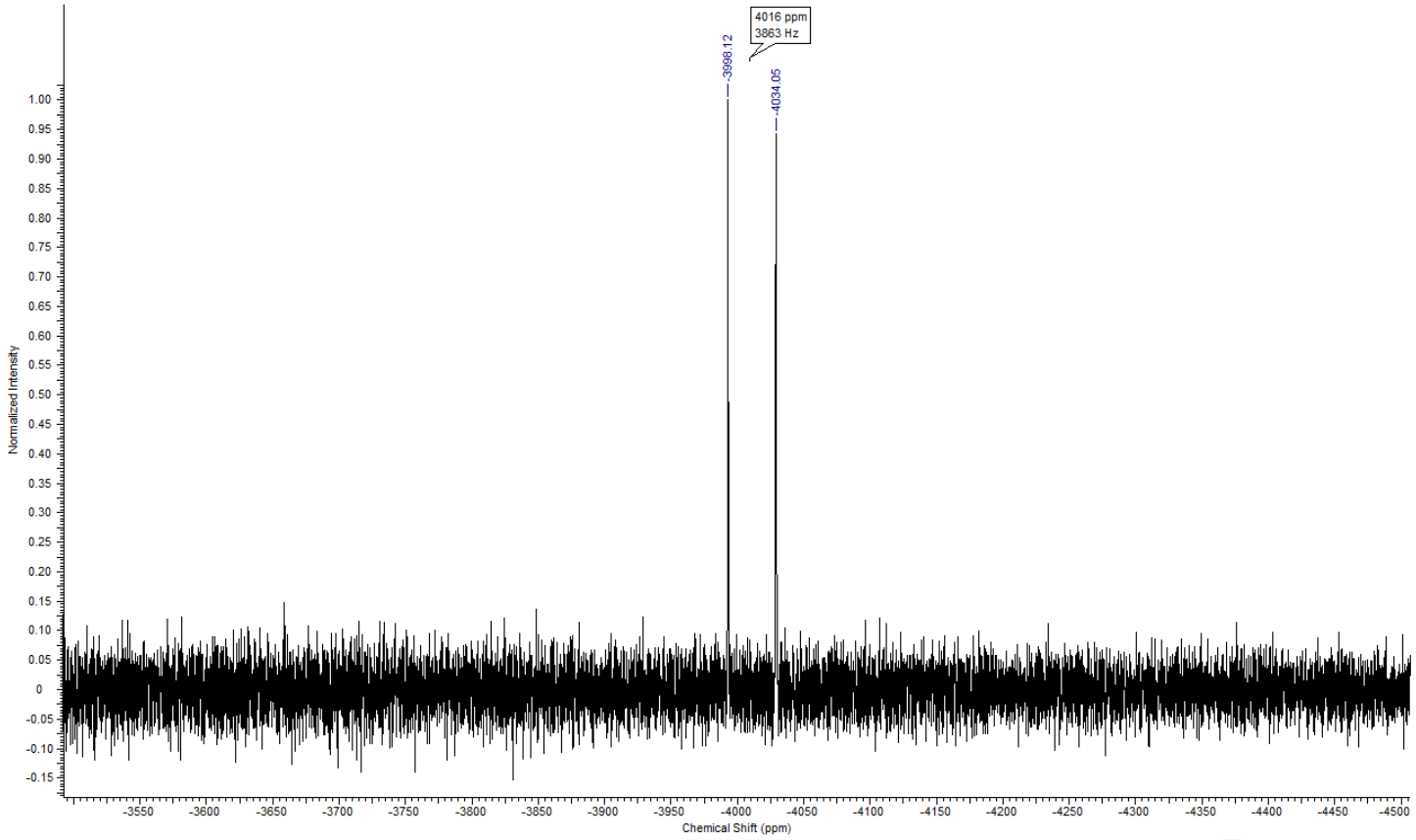

Fig. S 19: ^{195}Pt-NMR spectrum (108 MHz, $CDCl_3$) of complex **9b**.

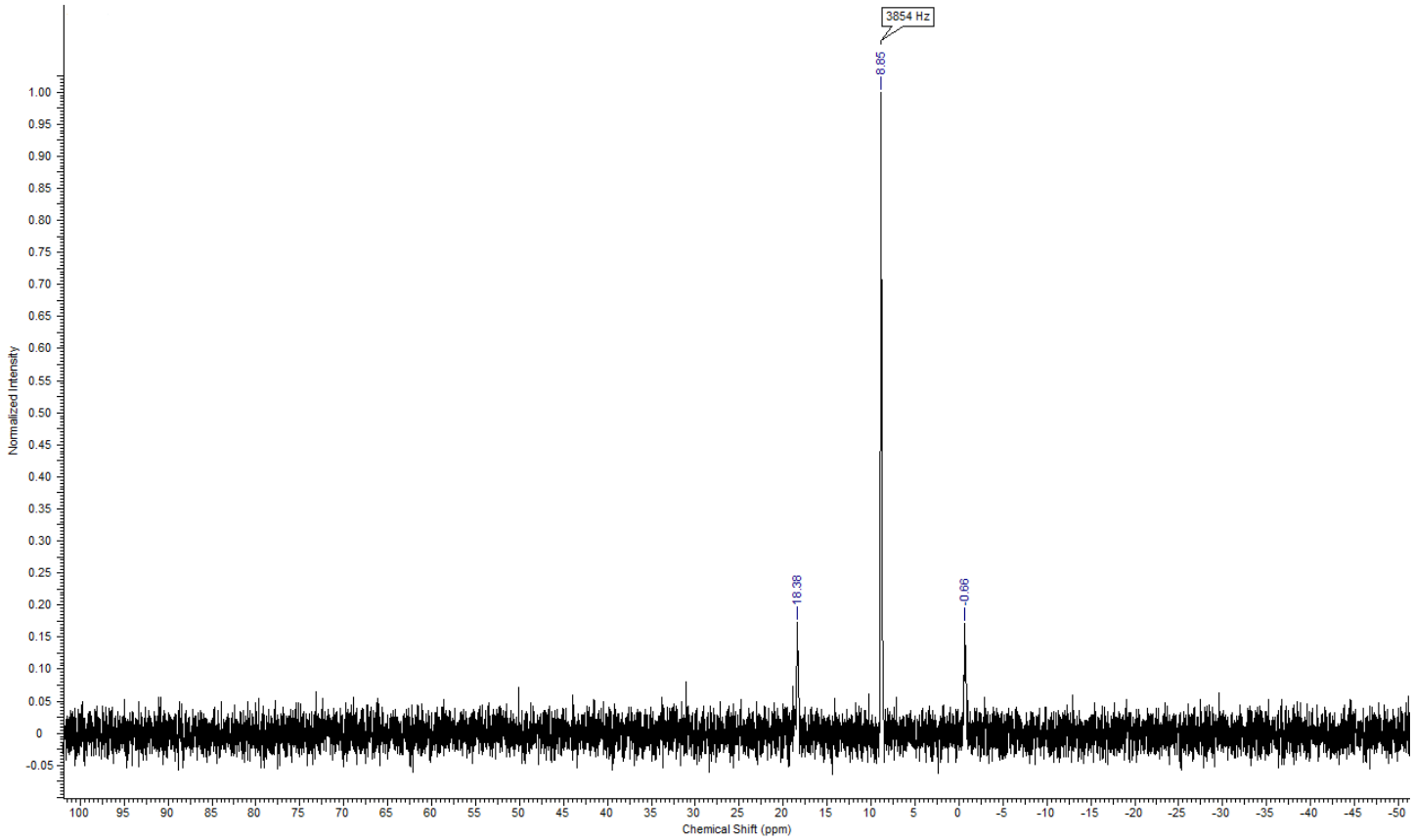

Fig. S 20: ^{31}P-NMR spectrum (202 MHz, $CDCl_3$) of complex **9b**.

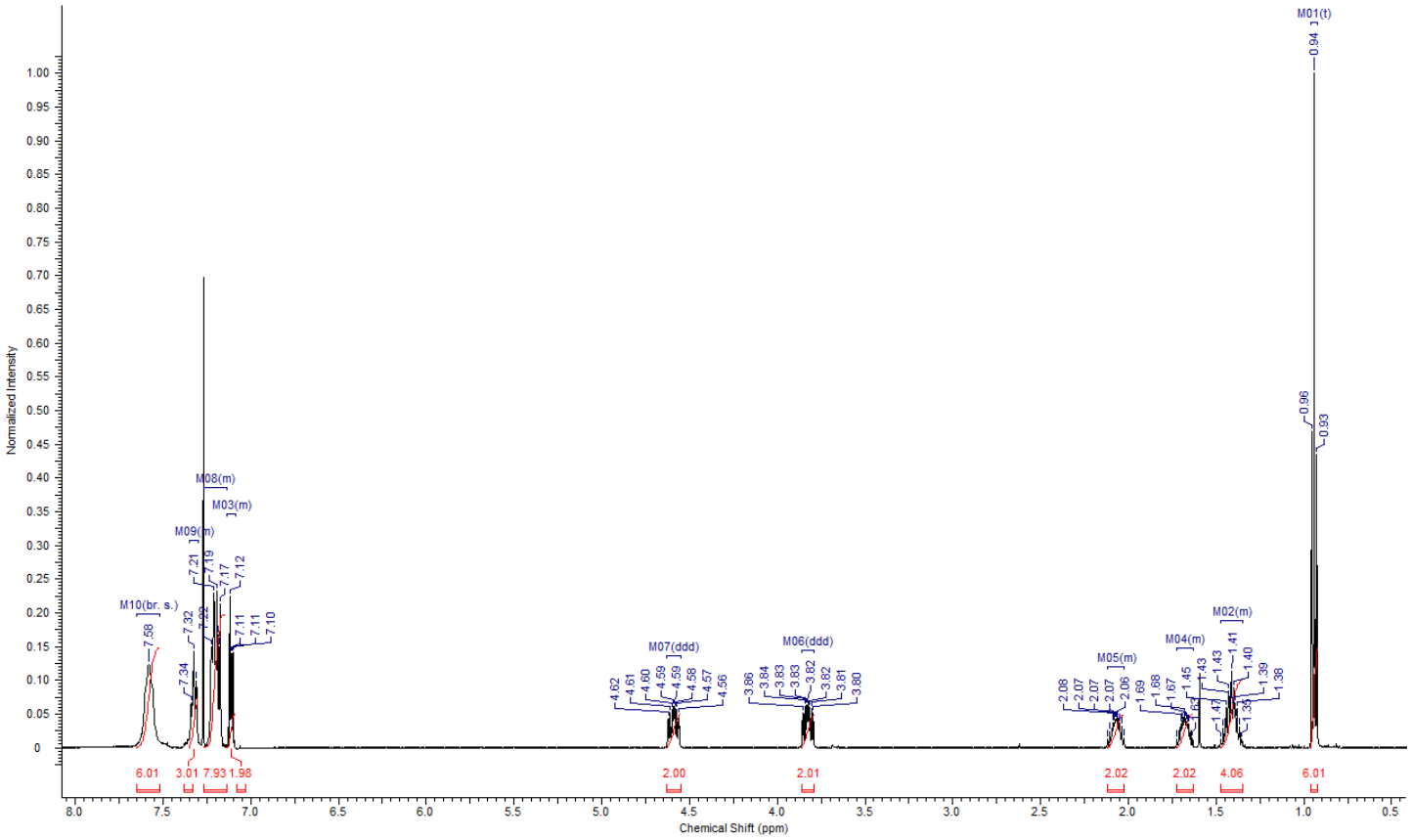

Fig. S 21: ^{1}H-NMR spectrum (500 MHz, $CDCl_3$) of complex **9c**.

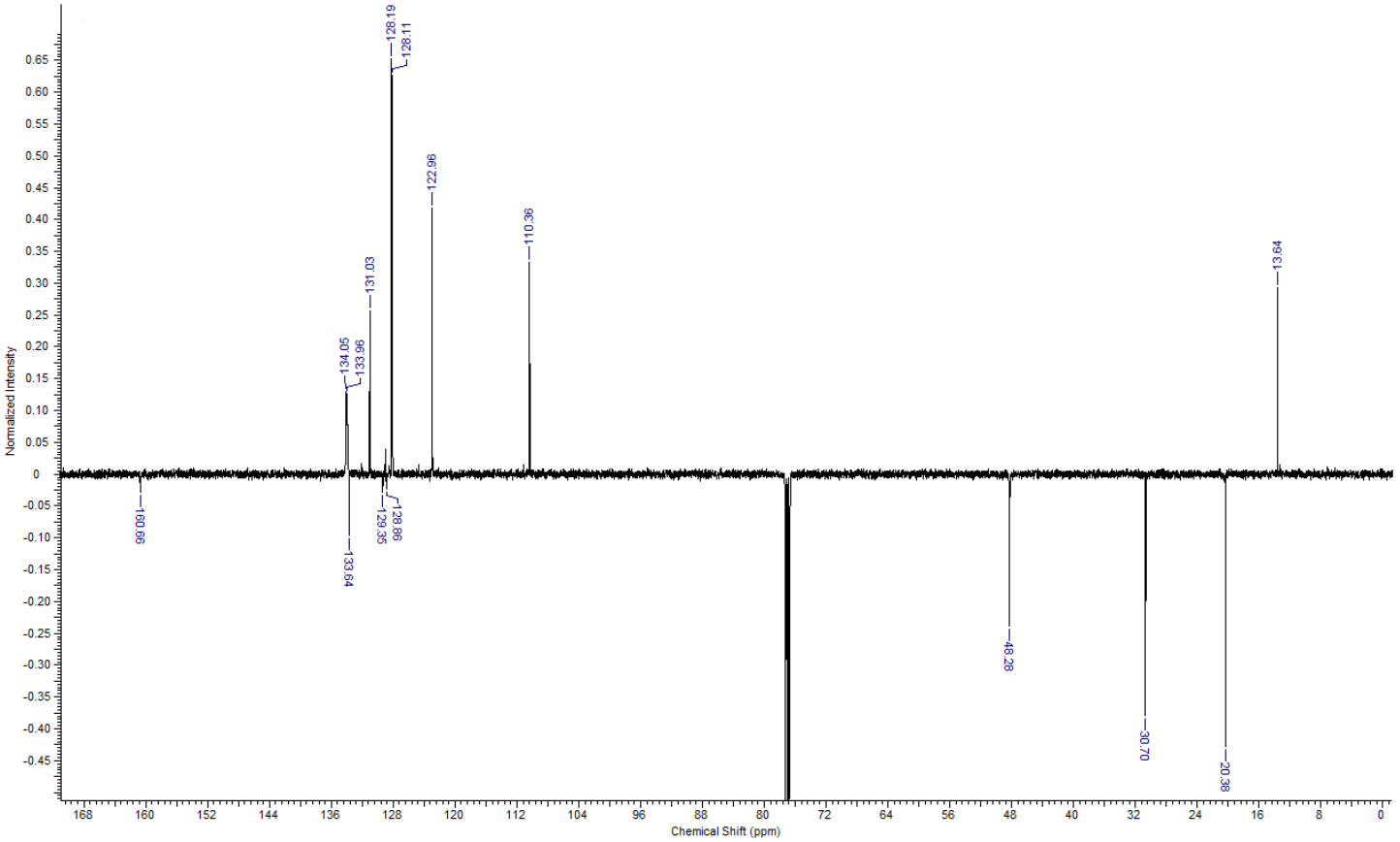

Fig. S 22: ^{13}C-NMR spectrum (126 MHz, $CDCl_3$) of complex **9c**.

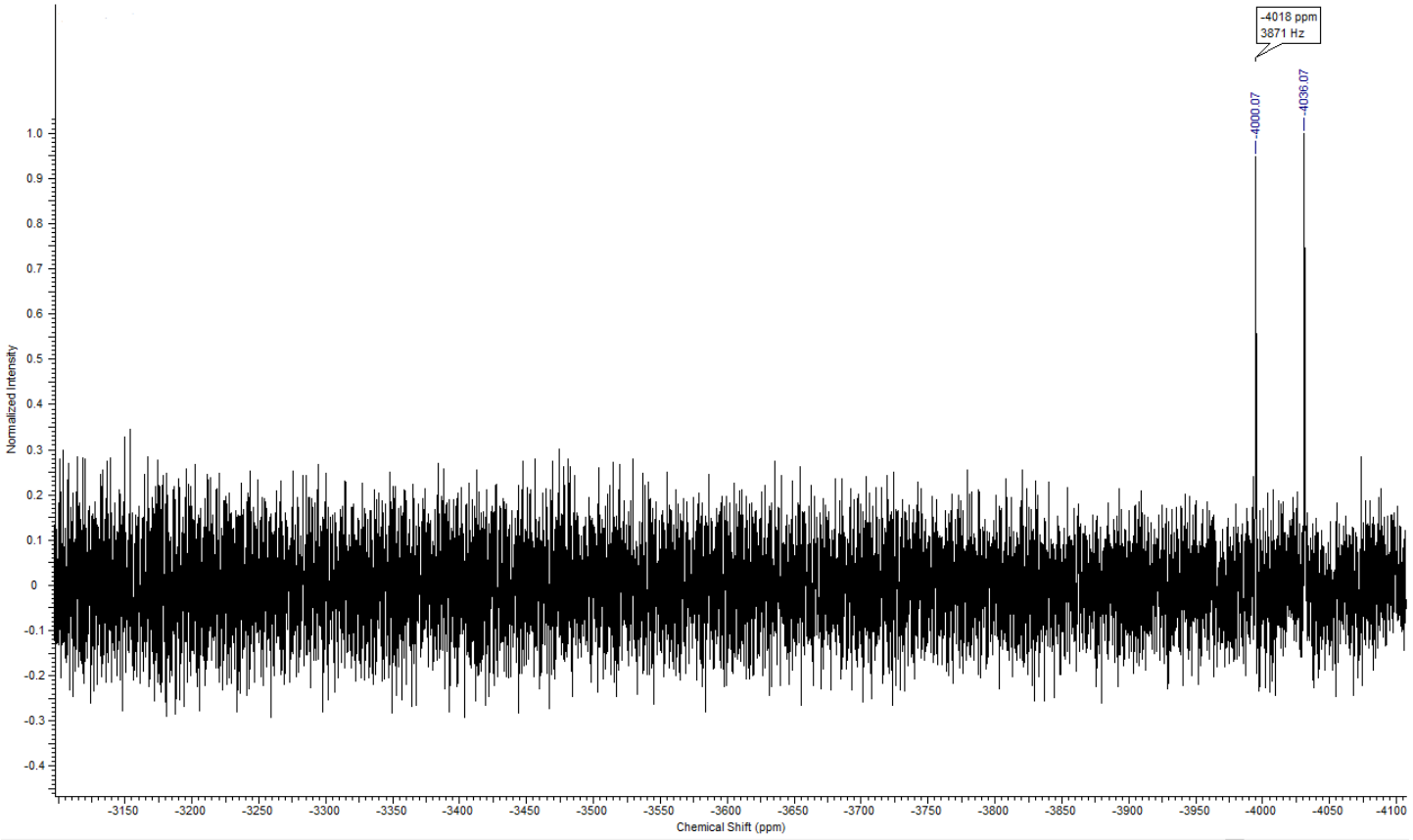

Fig. S 23: ^{195}Pt-NMR spectrum (108 MHz, $CDCl_3$) of complex **9c**.

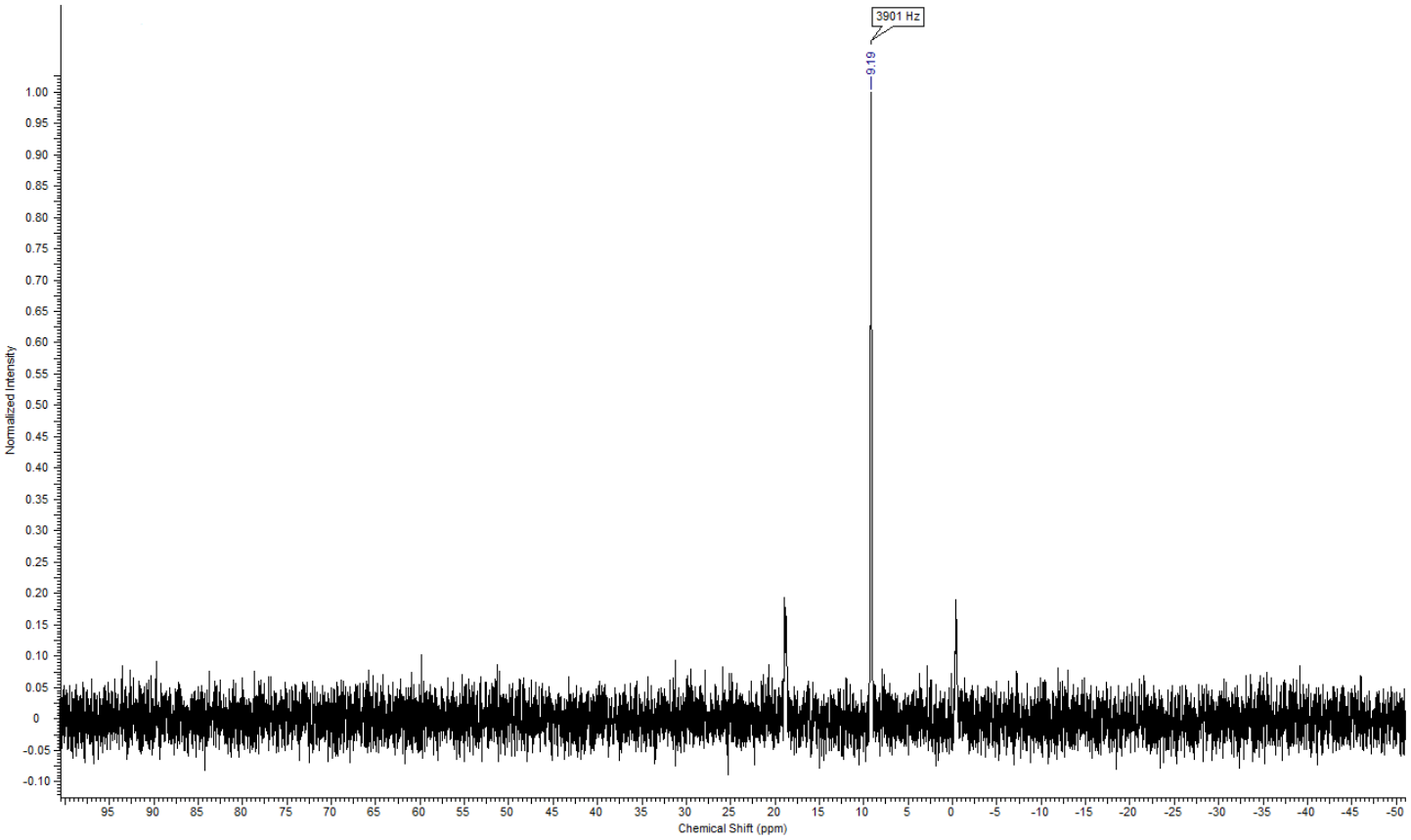

Fig. S 24: ^{31}P-NMR spectrum (202 MHz, $CDCl_3$) of complex **9c**.

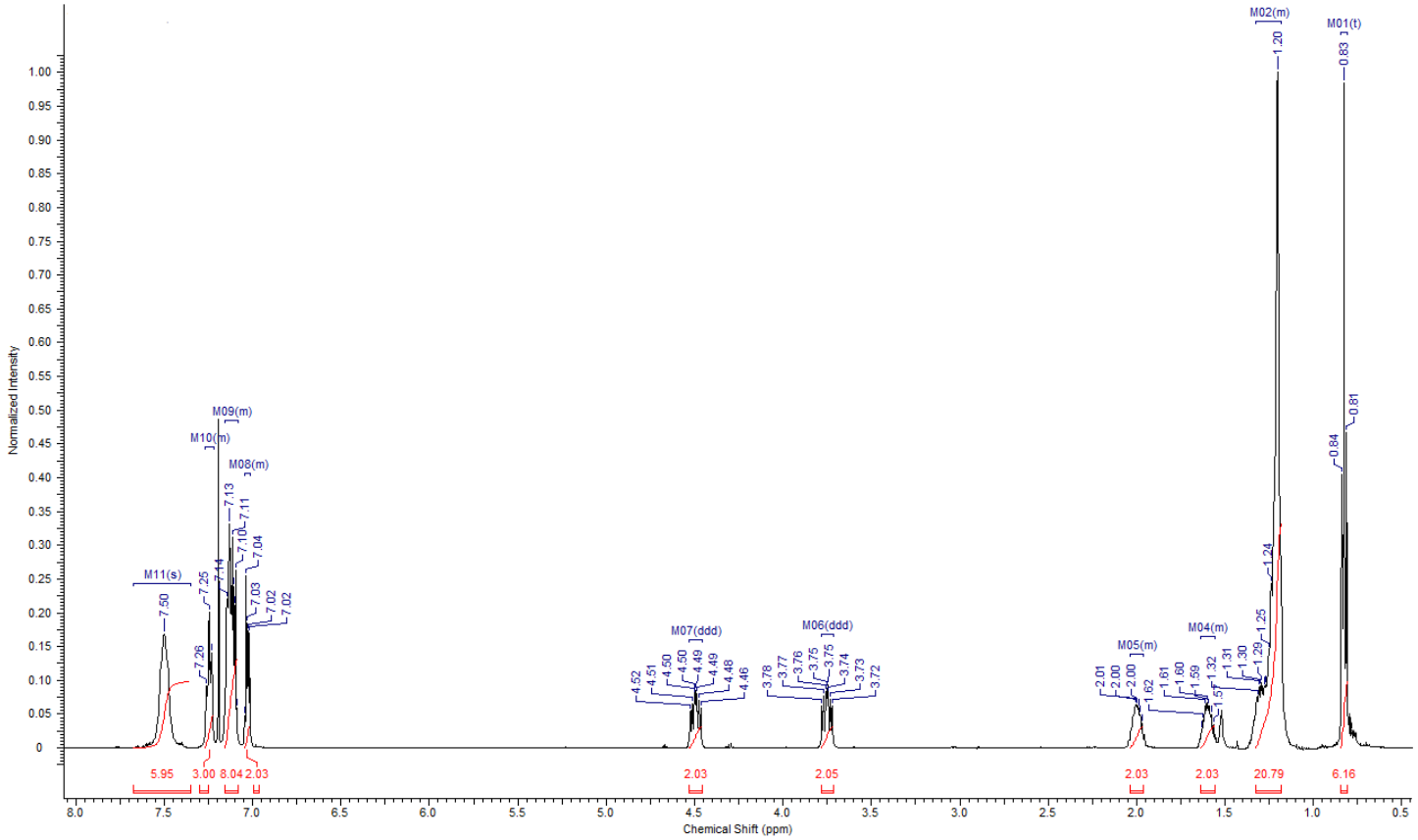

Fig. S 25: ^{1}H-NMR spectrum (500 MHz, $CDCl_3$) of complex **9d**.

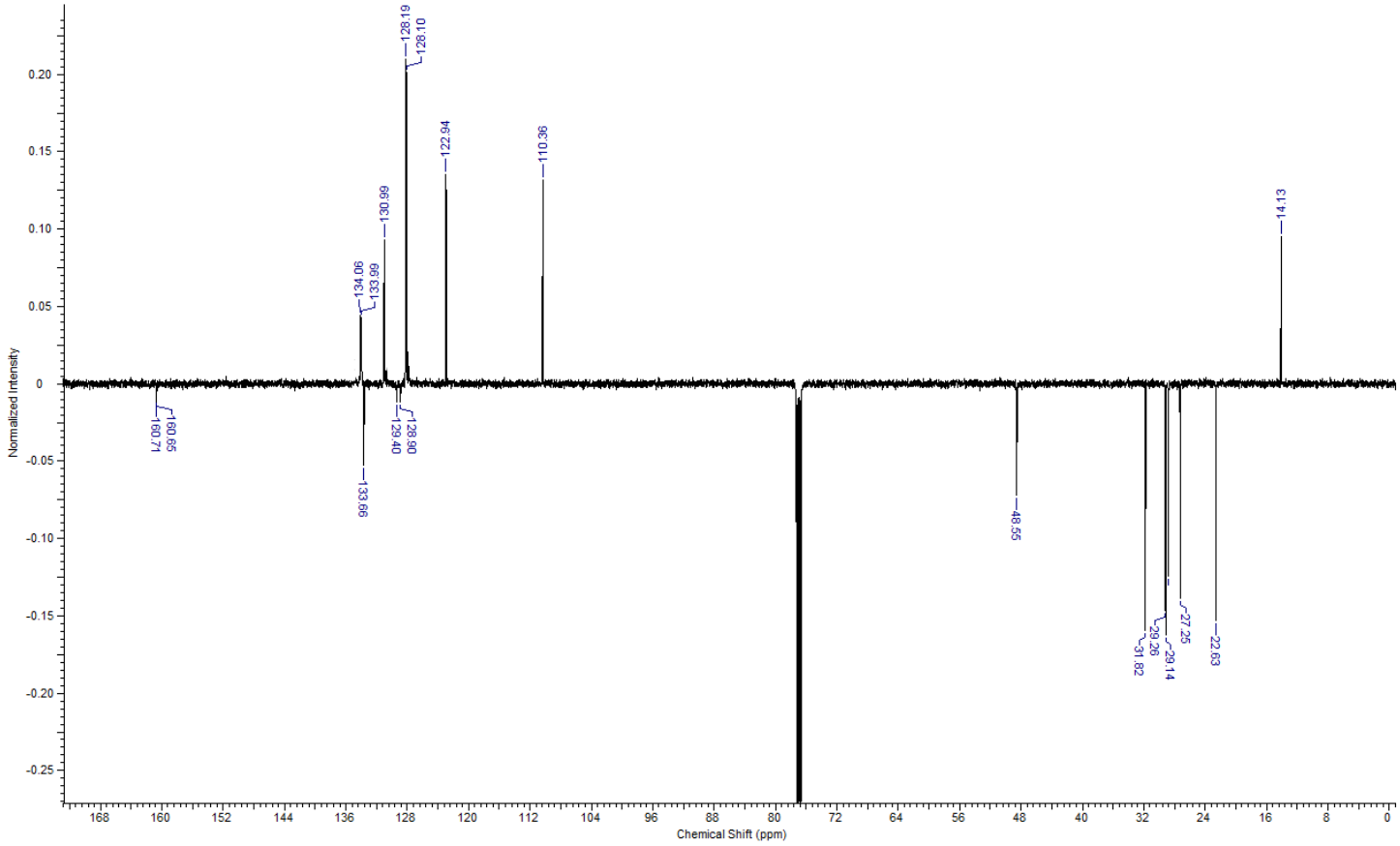

Fig. S 26: ^{13}C-NMR spectrum (126 MHz, $CDCl_3$) of complex **9d**.

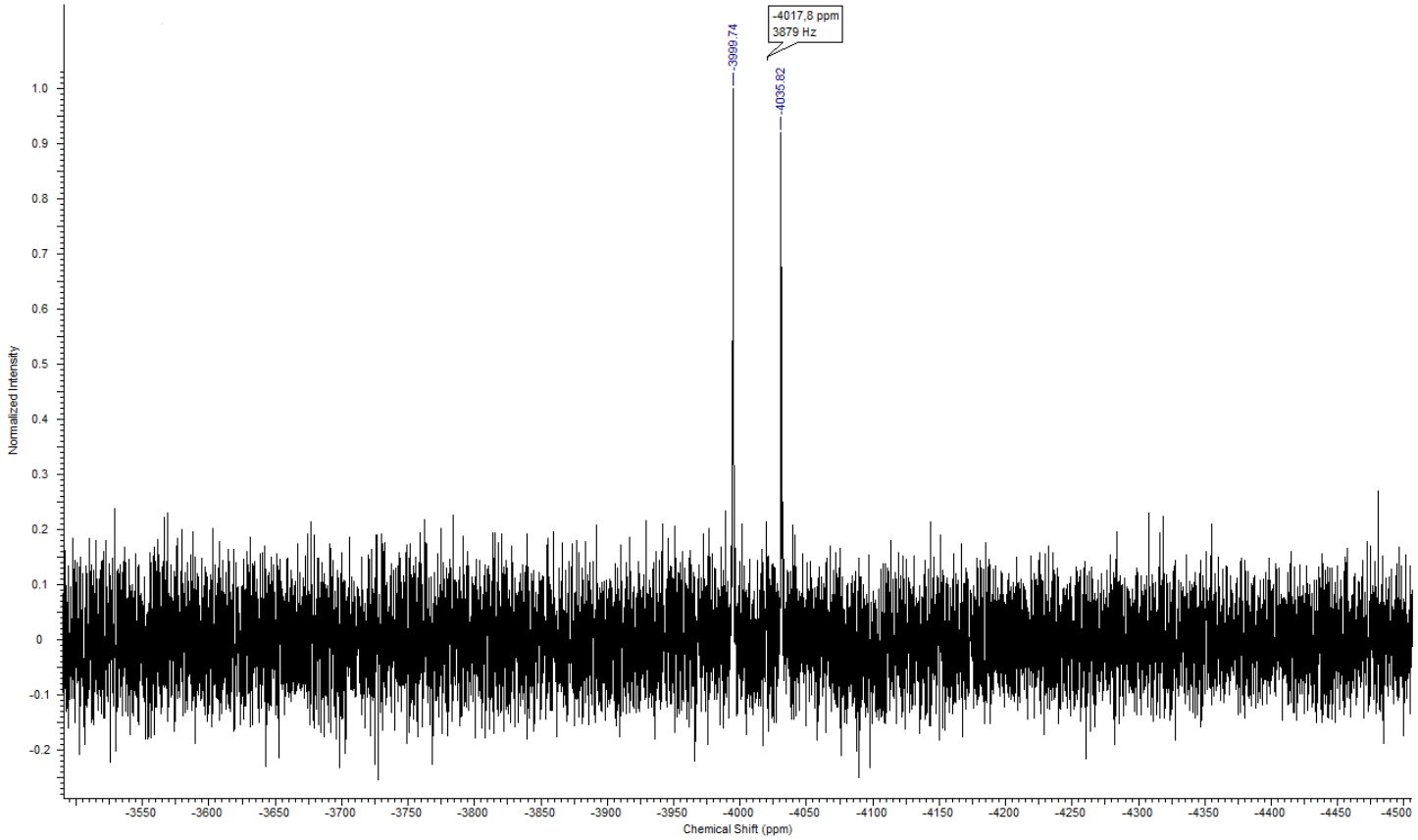

Fig. S 27: ^{195}Pt-NMR spectrum (108 MHz, $CDCl_3$) of complex **9d**.

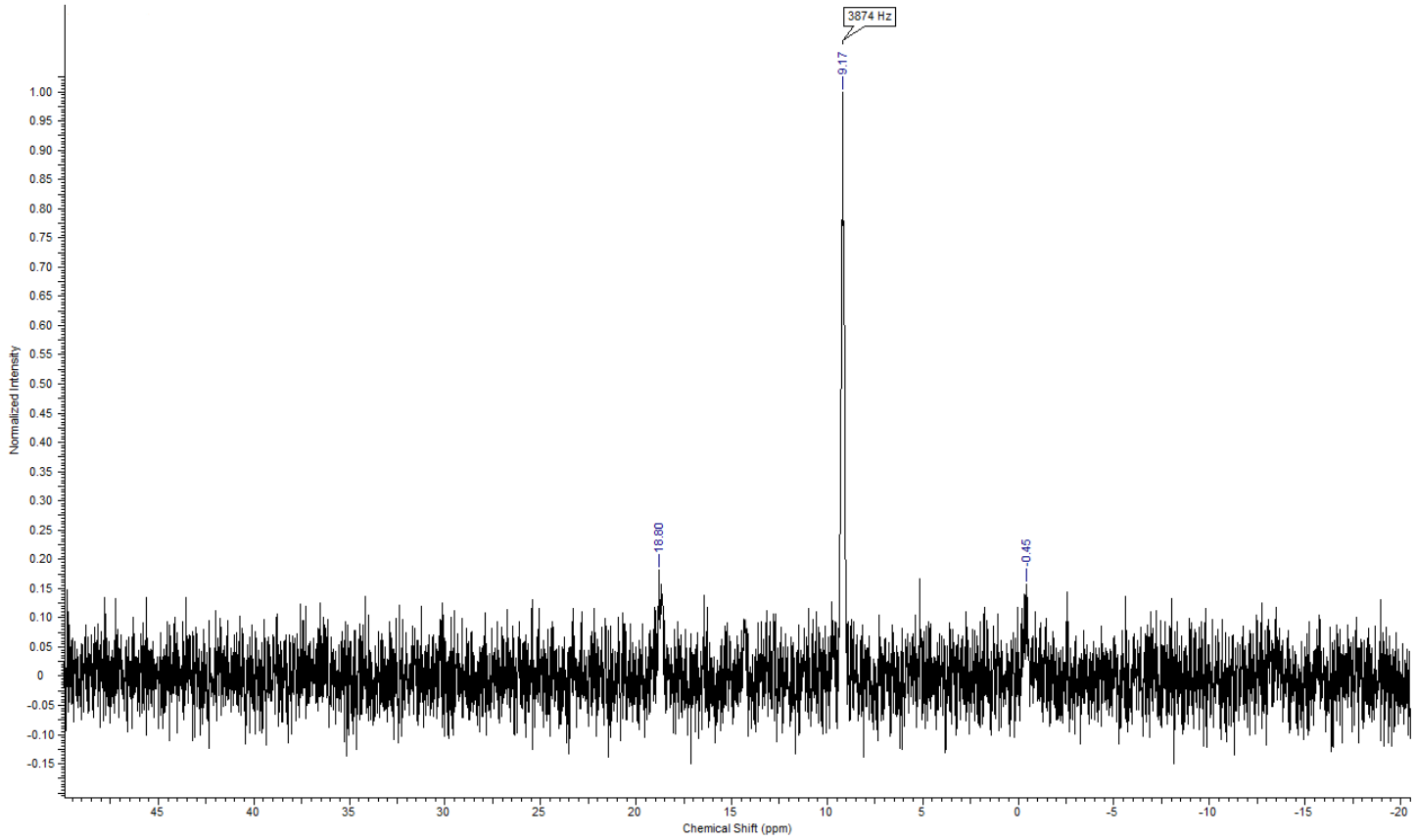

Fig. S 28: ^{31}P-NMR spectrum (202 MHz, $CDCl_3$) of complex **9d**.

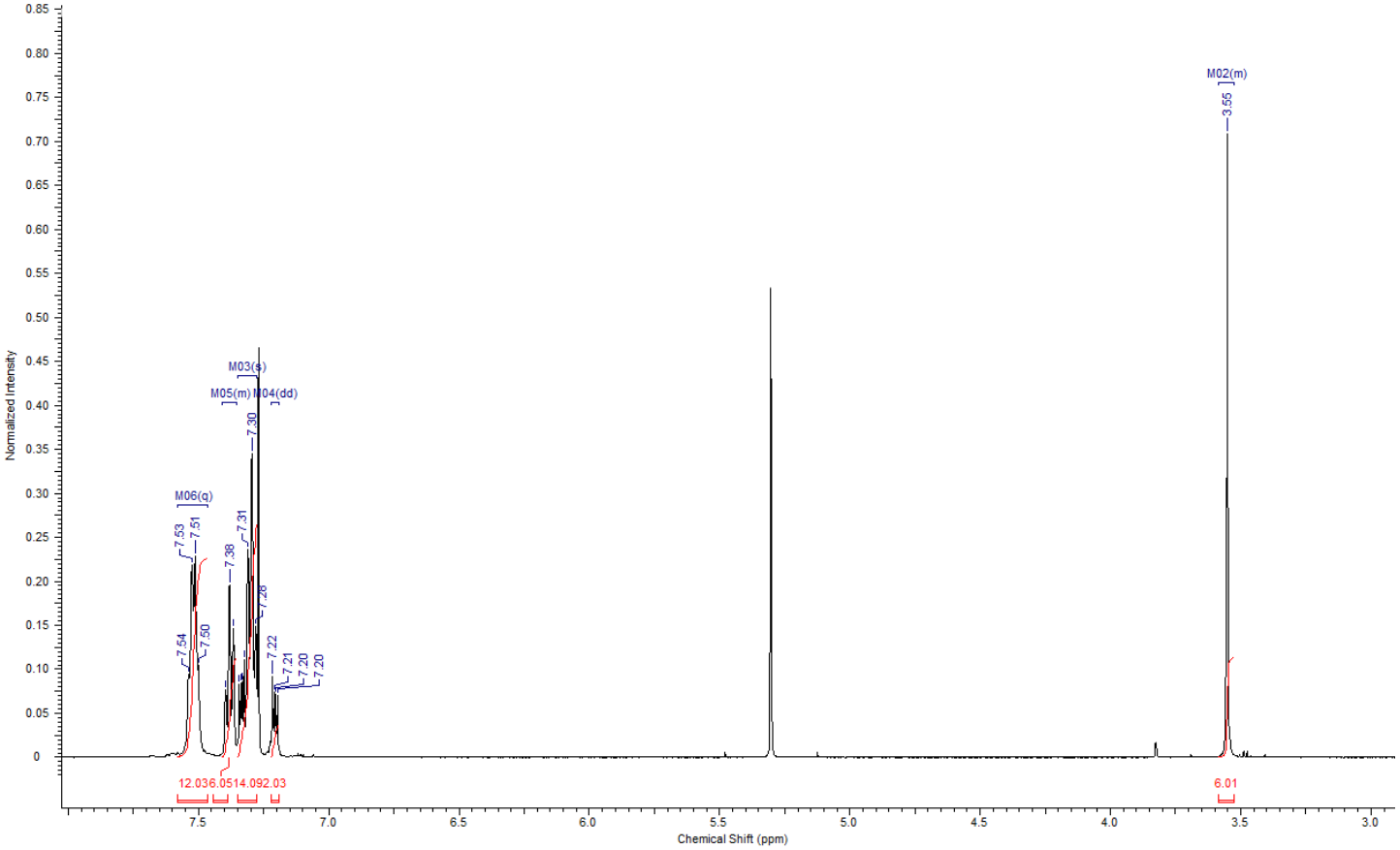

Fig. S 29: ^{1}H-NMR spectrum (500 MHz, $CDCl_3$) of complex **10a**.

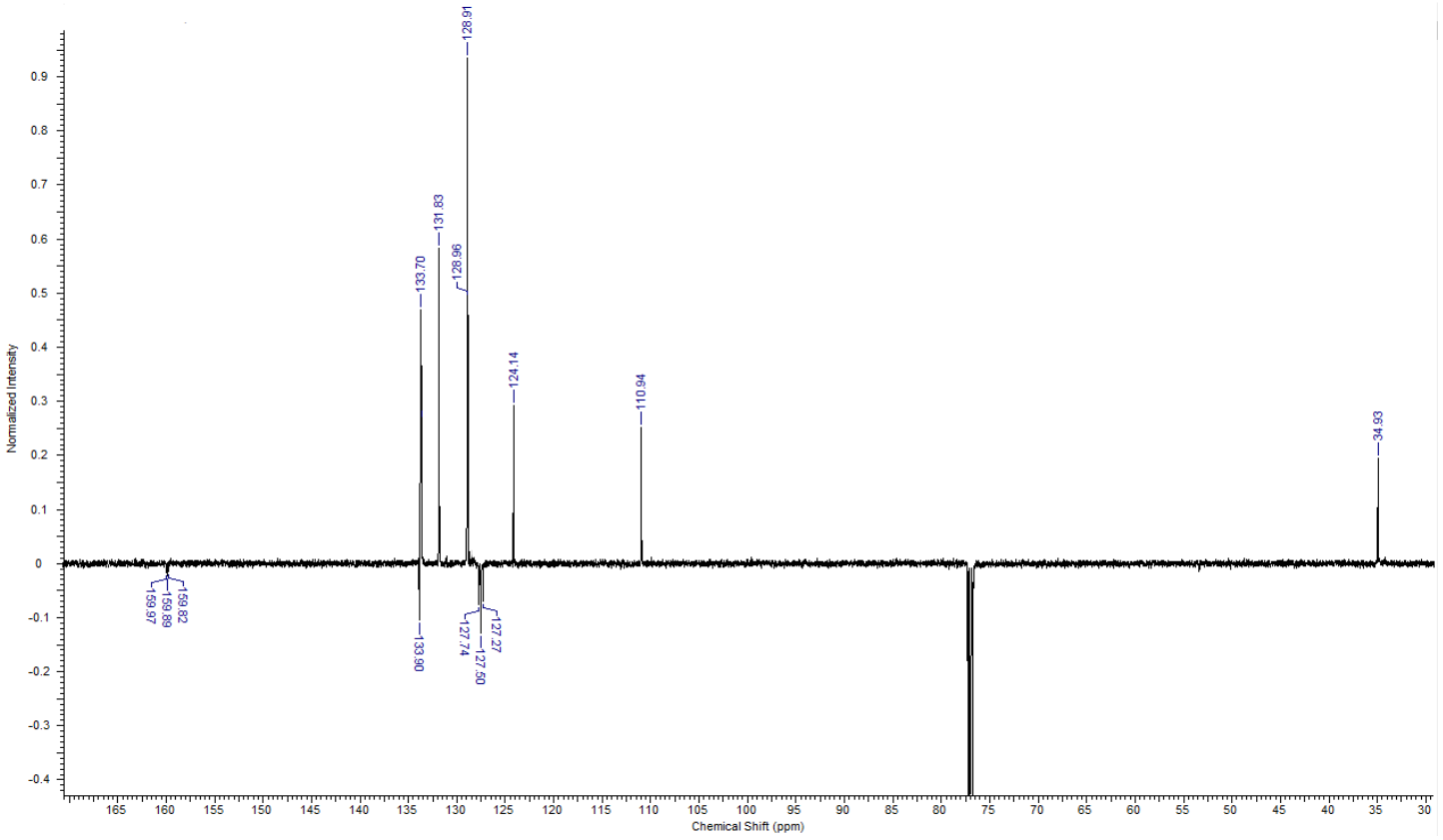

Fig. S 30: ^{13}C-NMR spectrum (126 MHz, $CDCl_3$) of complex **10a**.

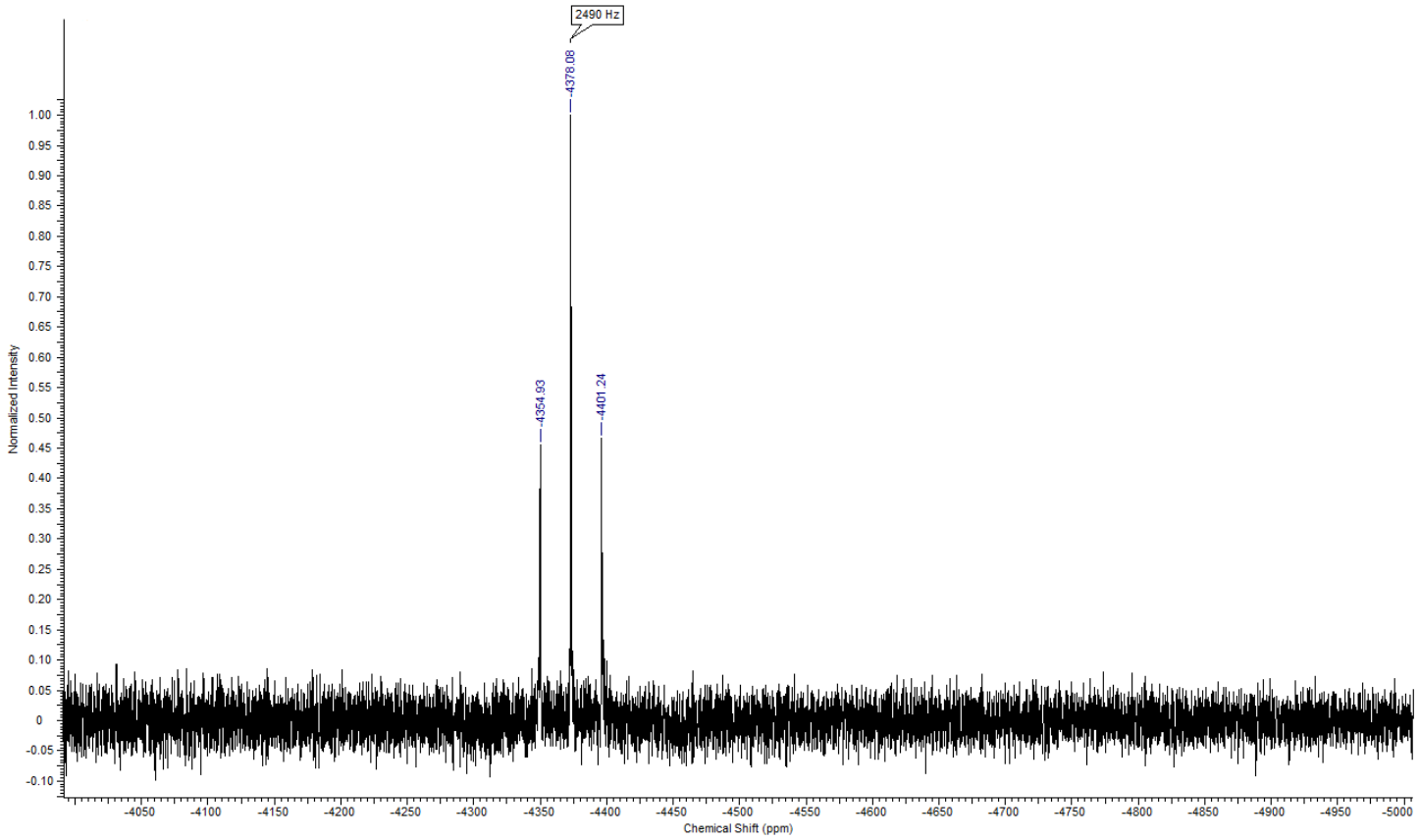

Fig. S 31: ^{195}Pt-NMR spectrum (108 MHz, $CDCl_3$) of complex **10a**.

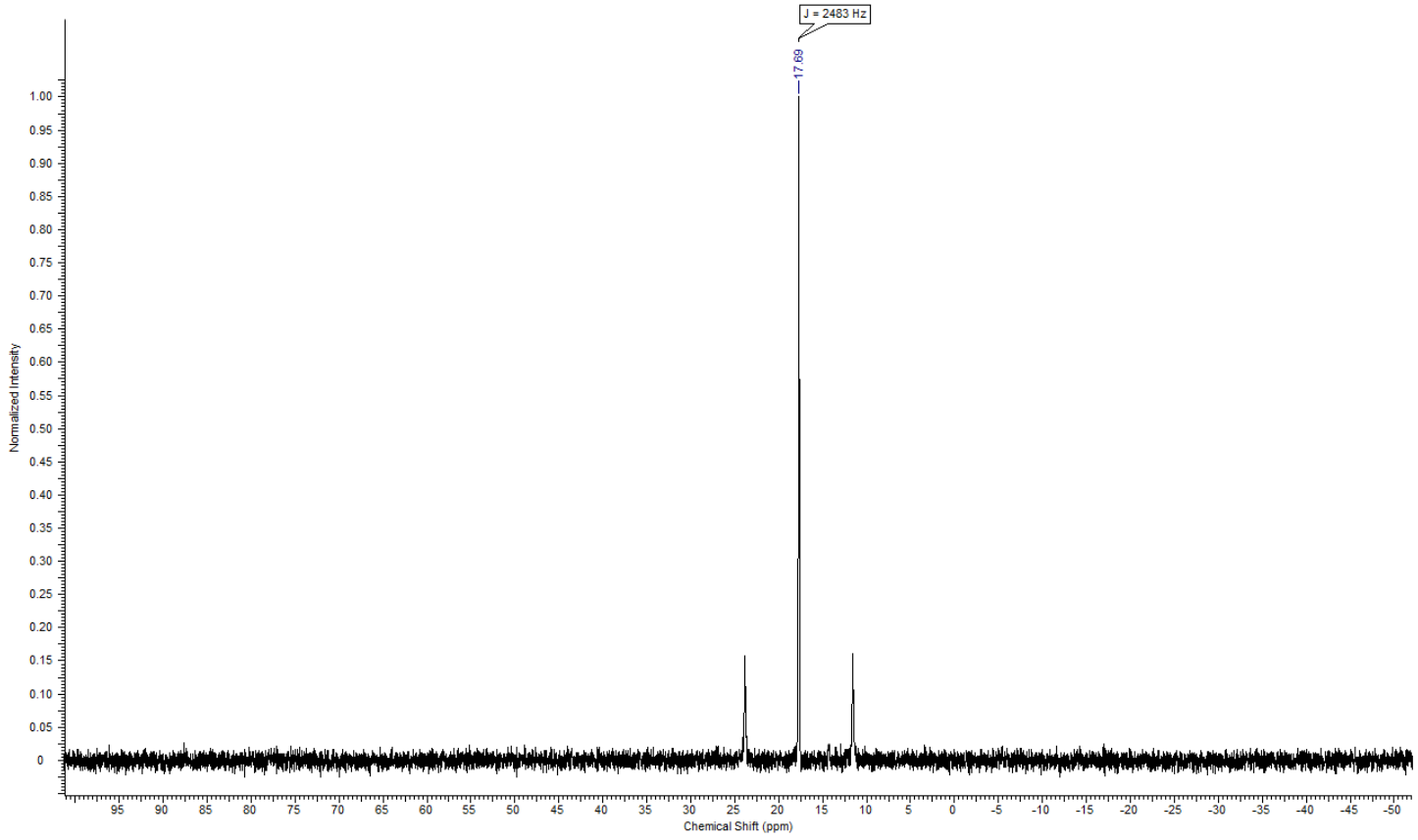

Fig. S 32: ^{31}P-NMR spectrum (202 MHz, $CDCl_3$) of complex **10a**.

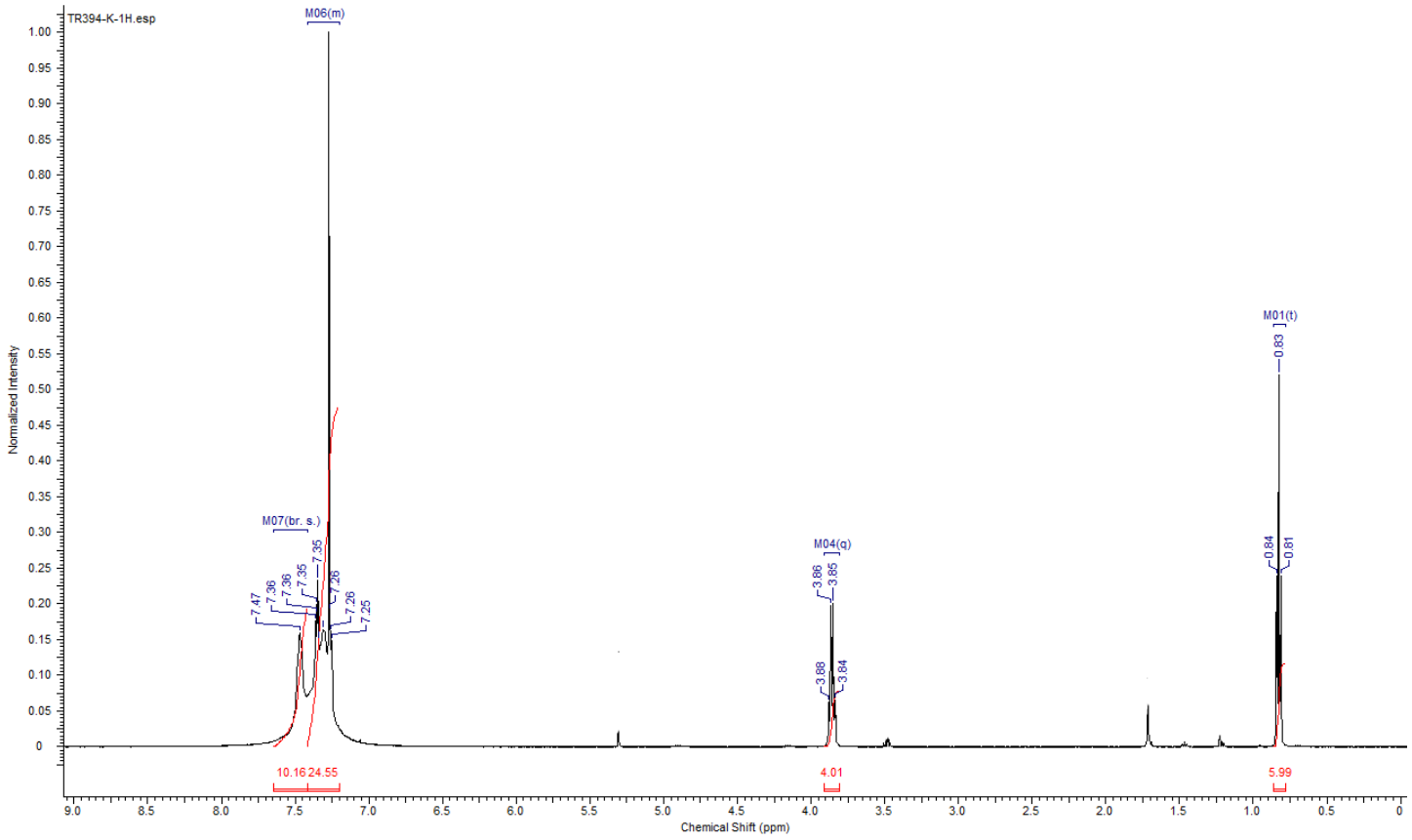

Fig. S 33: ^{1}H-NMR spectrum (500 MHz, $CDCl_3$) of complex **10b**.

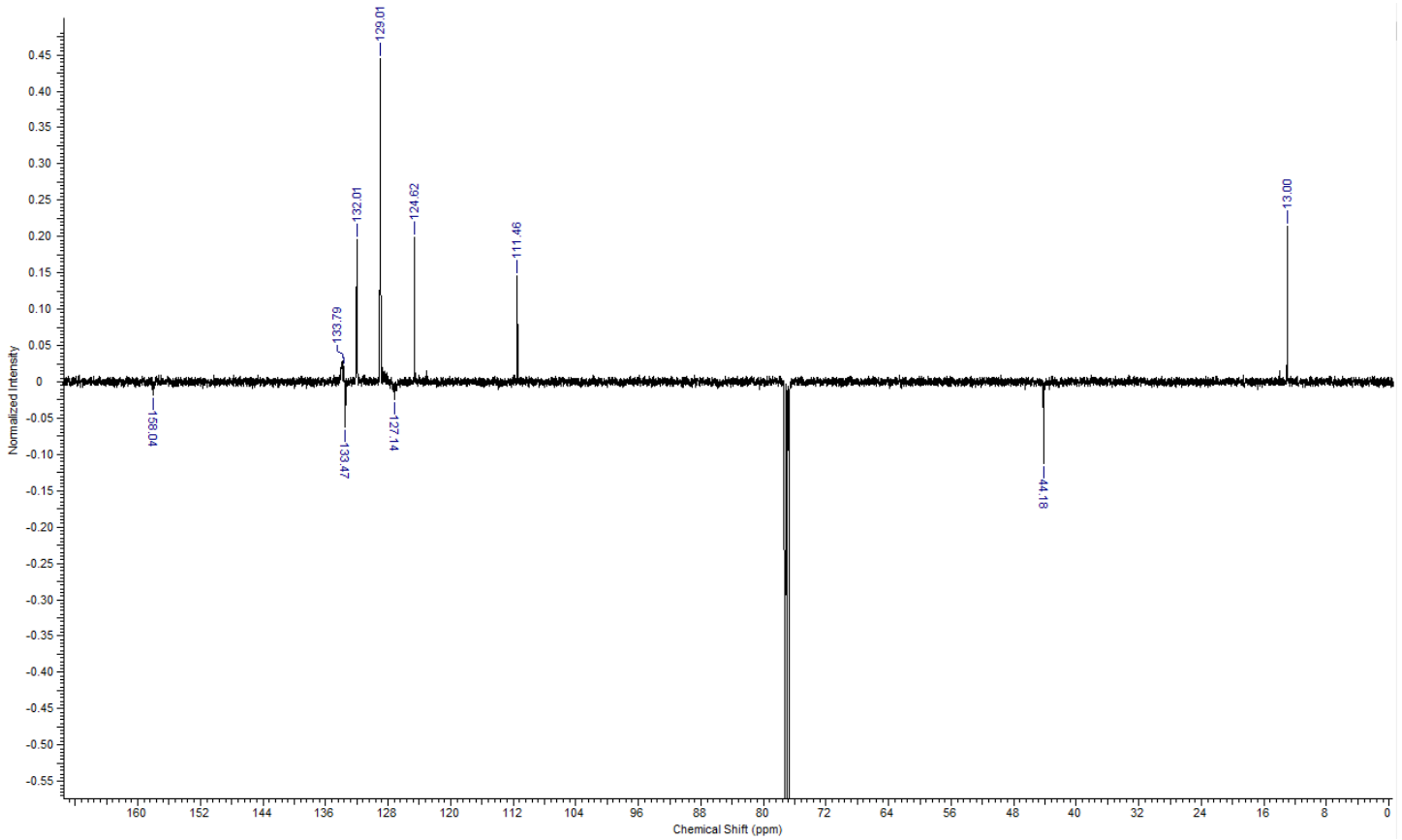

Fig. S 34: ^{13}C-NMR spectrum (126 MHz, $CDCl_3$) of complex **10b**.

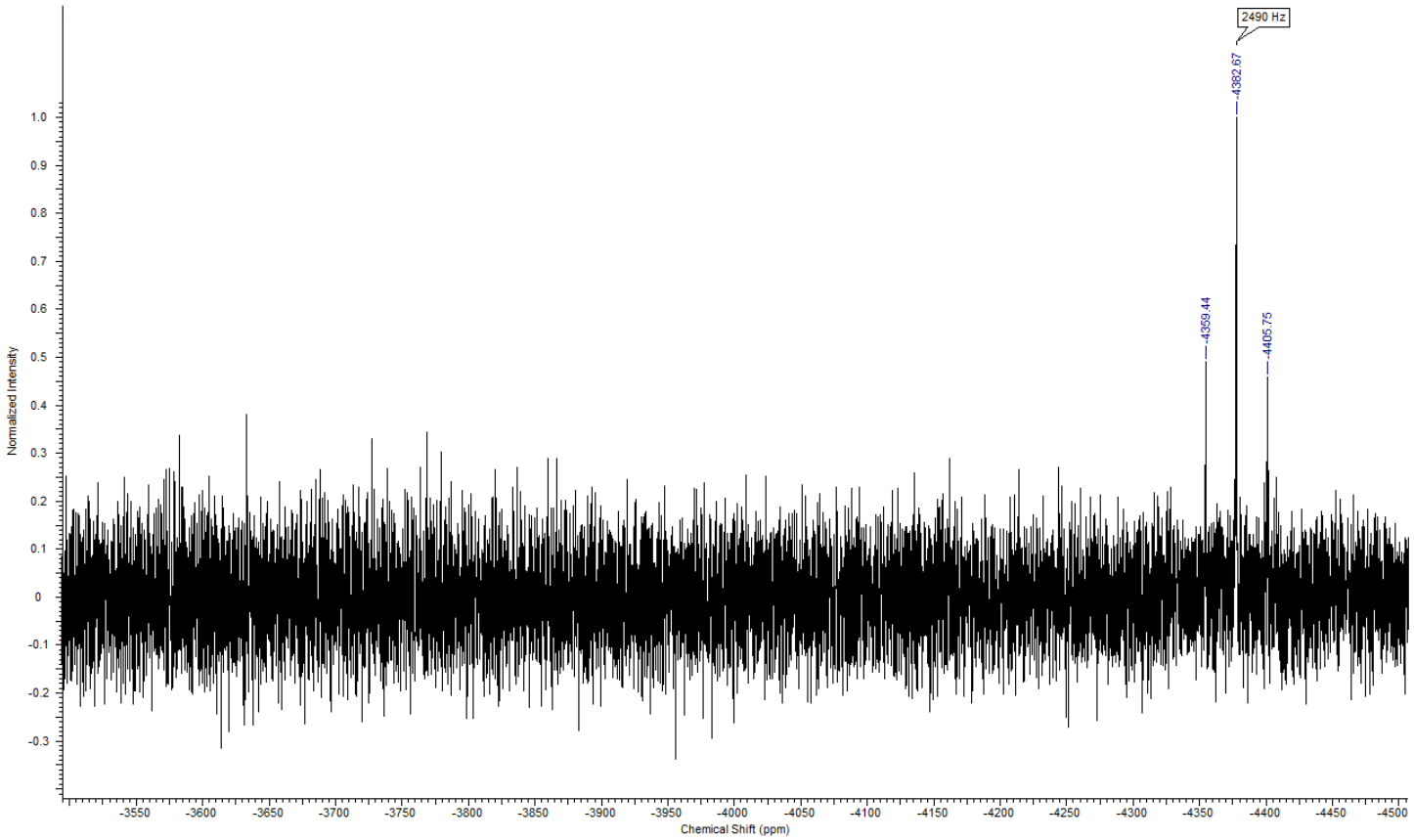

Fig. S 35: ^{195}Pt-NMR spectrum (108 MHz, $CDCl_3$) of complex **10b**.

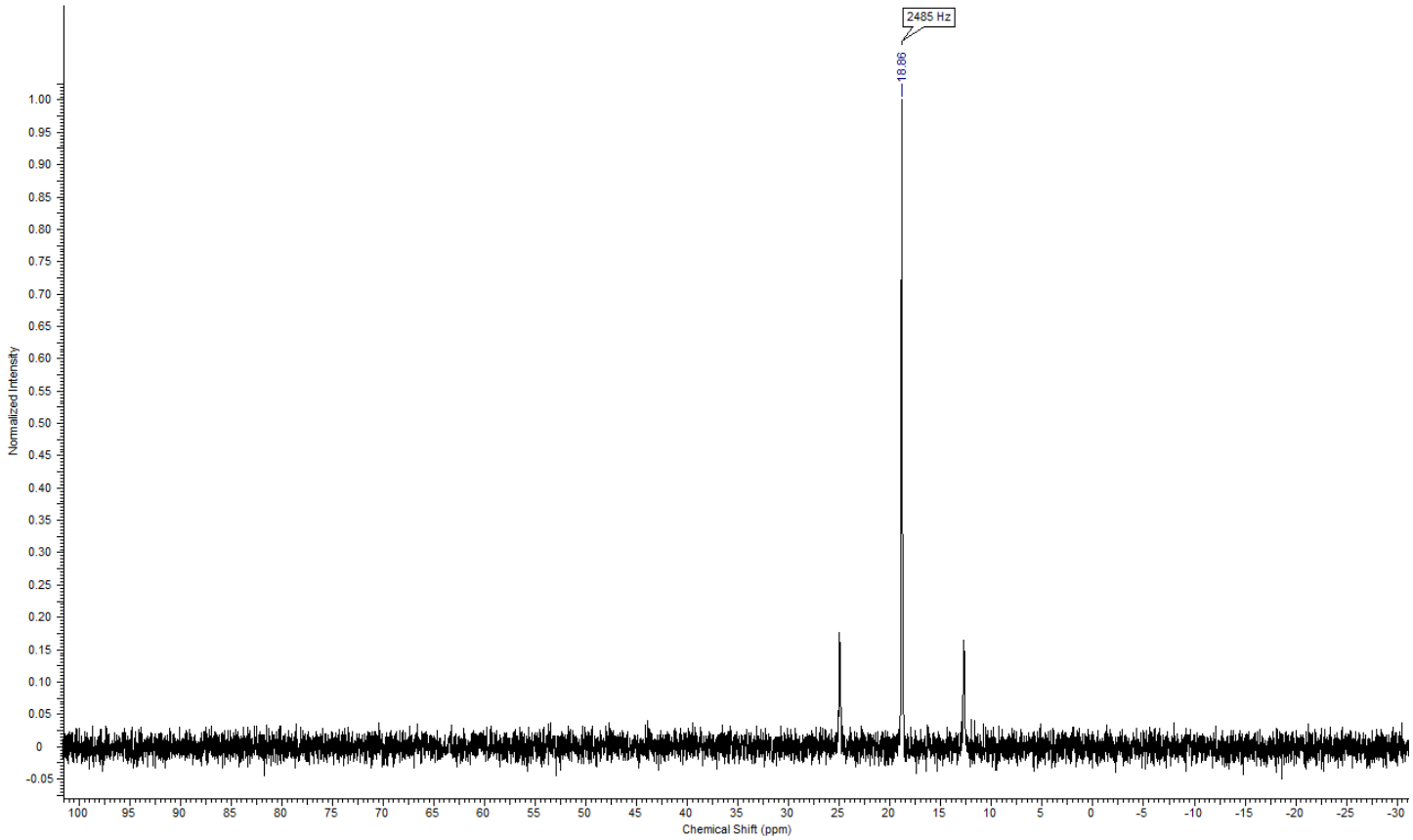

Fig. S 36: ^{31}P-NMR spectrum (202 MHz, $CDCl_3$) of complex **10b**.

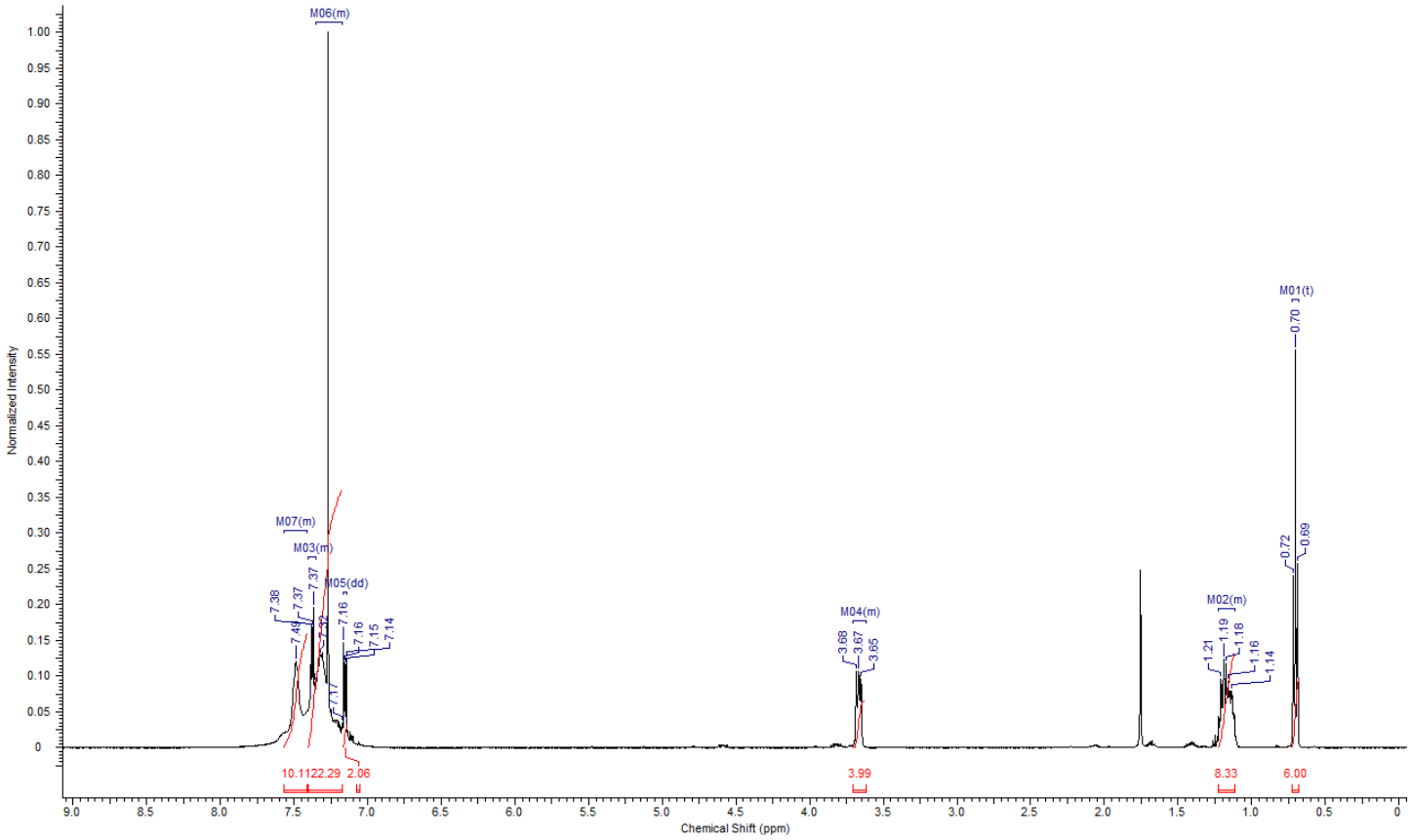

Fig. S 37: ^{1}H-NMR spectrum (500 MHz, $CDCl_3$) of complex **10c**.

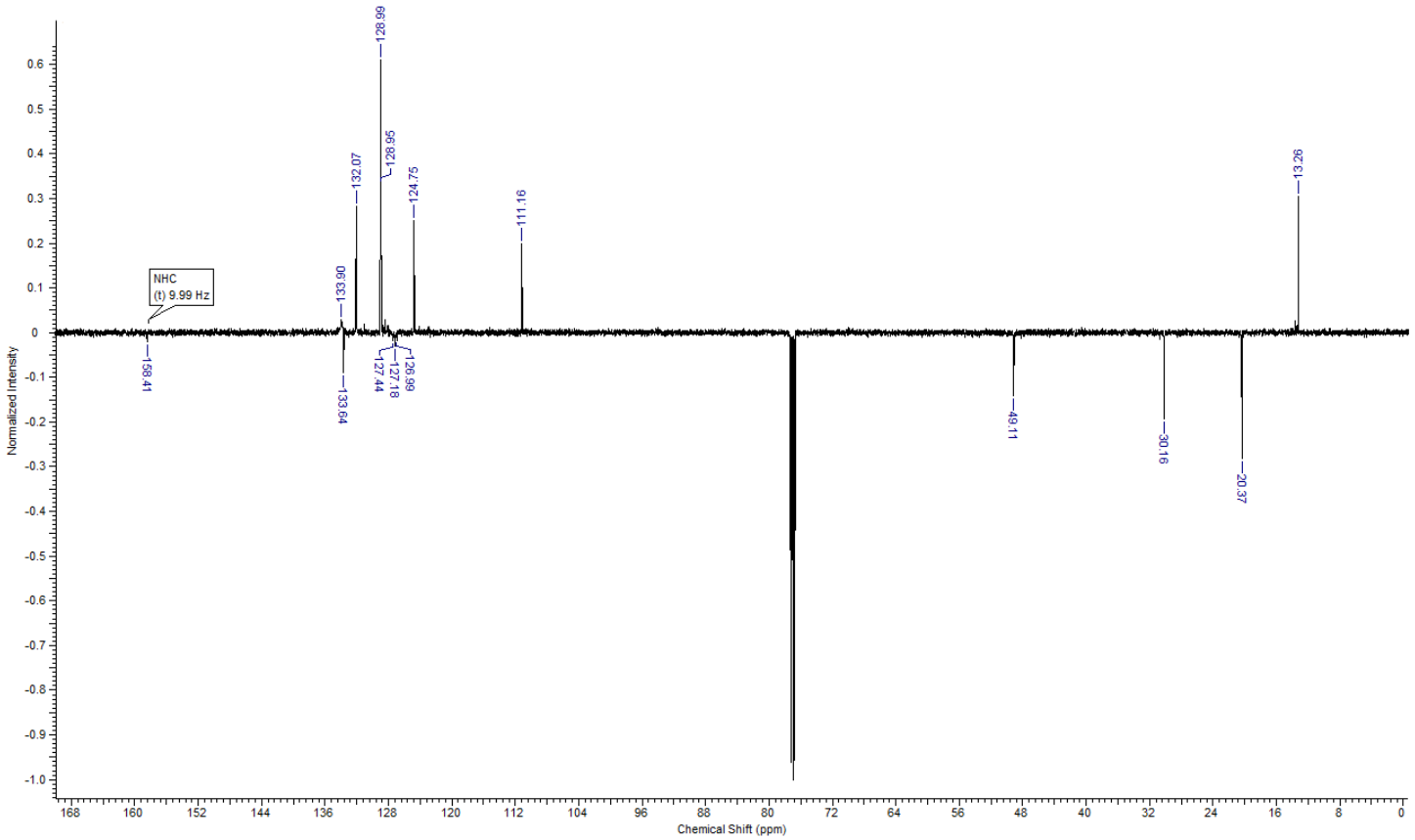

Fig. S 38: ^{13}C-NMR spectrum (126 MHz, $CDCl_3$) of complex **10c**.

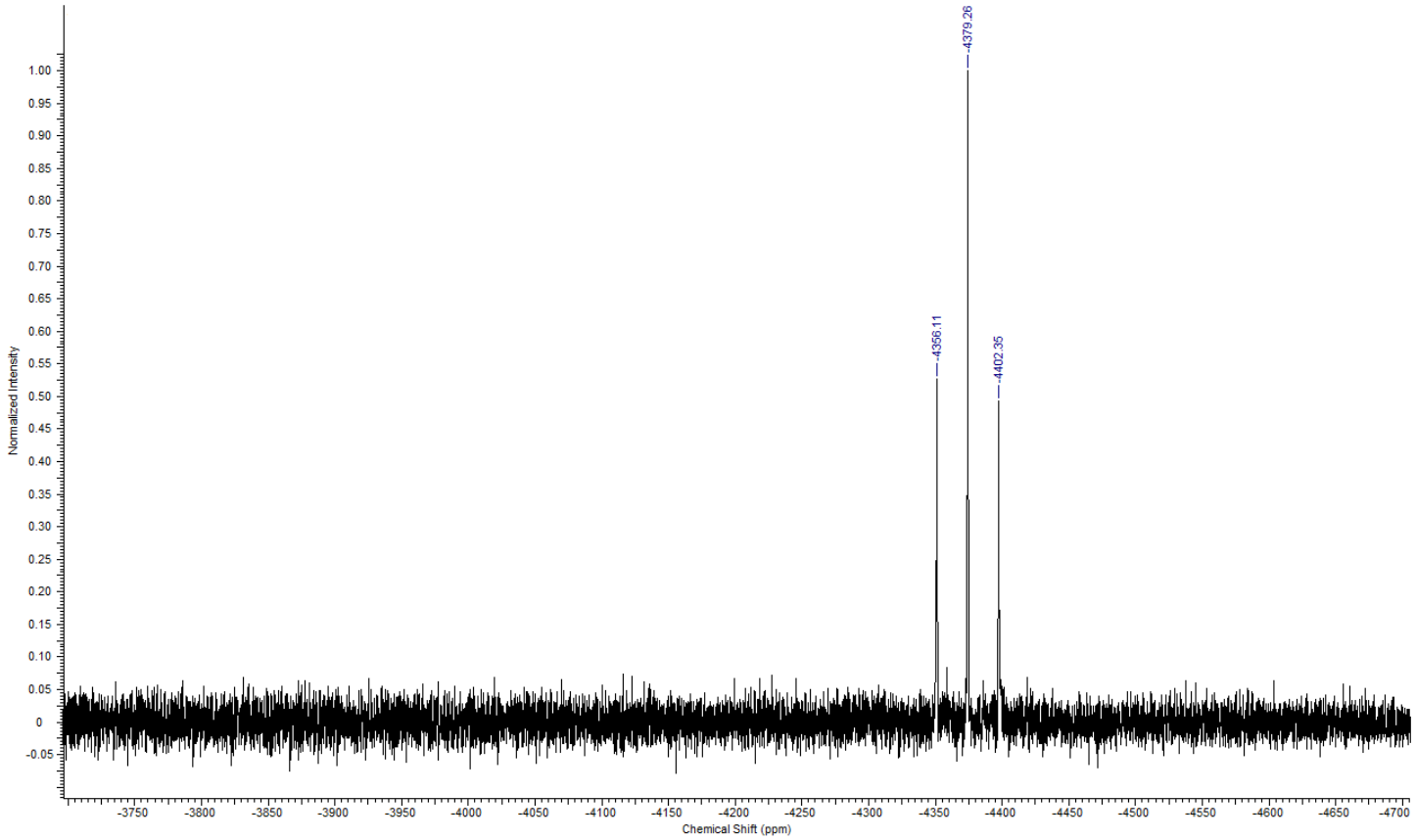

Fig. S 39: ^{195}Pt-NMR spectrum (108 MHz, $CDCl_3$) of complex **10c**.

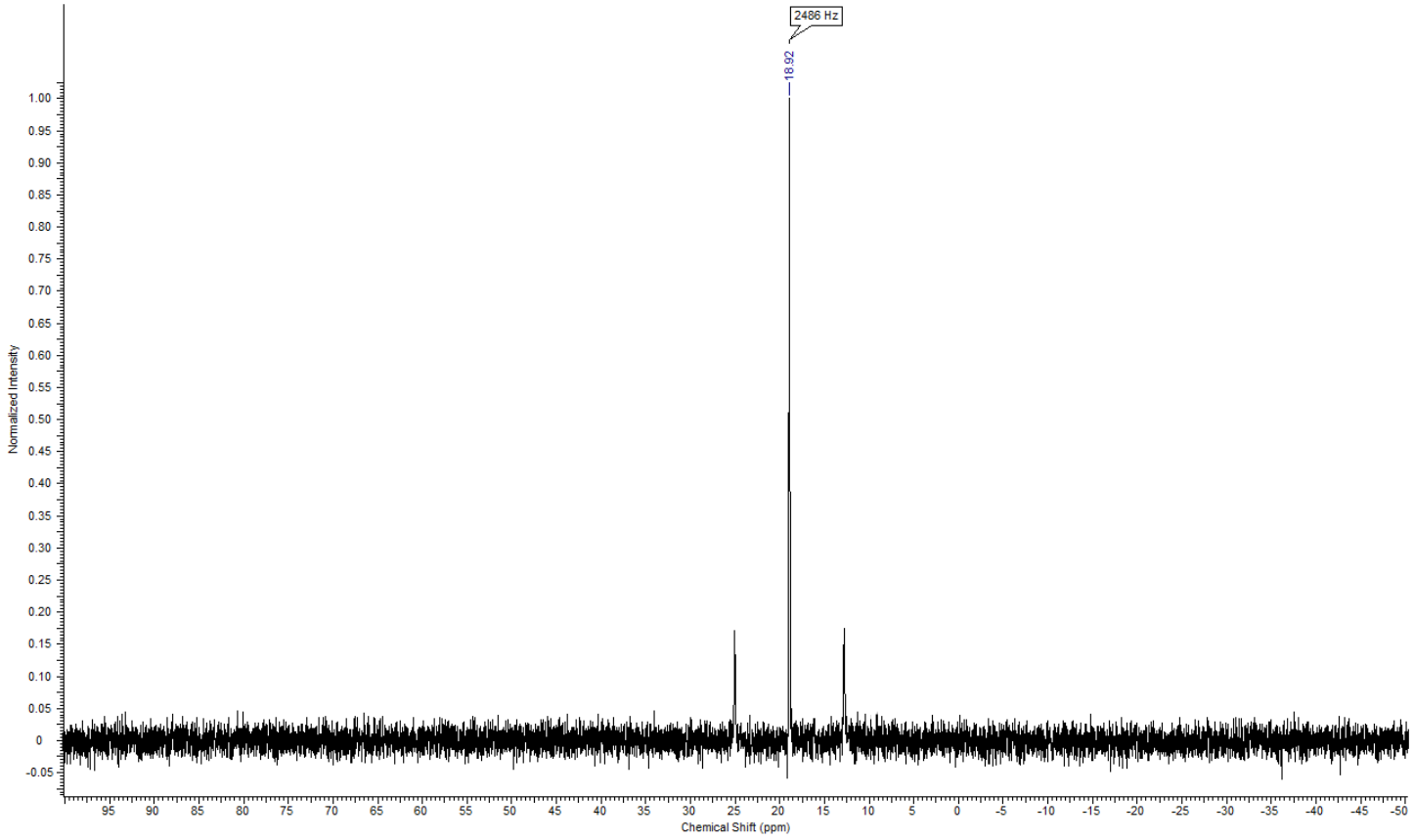

Fig. S 40: ^{31}P-NMR spectrum (202 MHz, $CDCl_3$) of complex **10c**.

Table S 41. Cellular accumulation of cisplatin and tested complexes in HCT116 cells.[a]

Compound	pmolPt/10^6cells
CDDP	49 ± 3
8a	67 ± 5
8b	88 ± 12
8c	97 ± 2
9a	122 ± 21
9b	245 ± 18
9c	316 ± 22
9d	59 ± 4
10a	520 ± 27
10b	555 ± 21
10c	592 ± 59

[a]Cellular accumulation of Pt from tested compounds (8 μM in media) in HCT116 cells after 5 h of treatment. Each value in the table is in pmol Pt/10^6 cells. The results are expressed as the mean ± SD of three independent experiments.

Table S 3. Binding of **8c**, **9c**, **10a-c** to synthetic polydeoxyribonucleotides determined by FAAS.

	8c	**9c**	**10a**	**10b**	**10c**
poly (dA)	35%	40%	22%	20%	15%
poly (dC)	5%	3%	1%	1%	2%
poly (dG)	75%	82%	55%	52%	49%
poly (dT)	0.1%	0%	0.3%	0.1%	0.5%

Binding (%) was calculated as a ratio of Pt associated with the polydeoxyribonucleotides after dialysis to the total amount of Pt present in the sample, multiplied by 100.

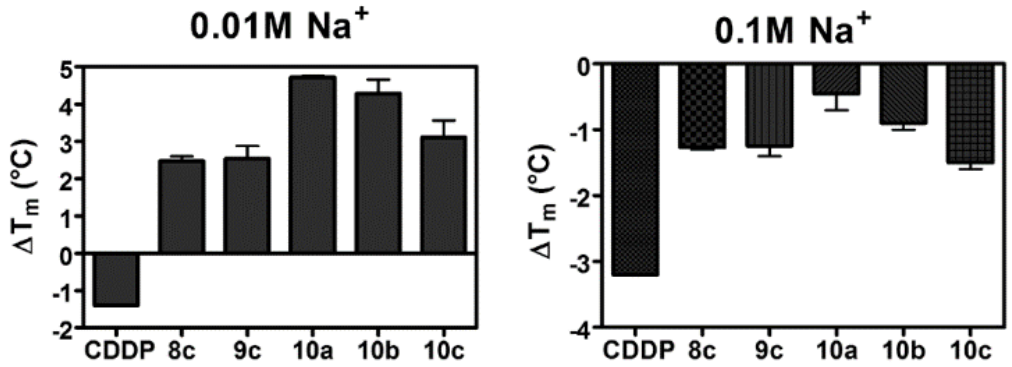

Fig. S 41. ΔT_m values of ct DNA modified by **CDDP**, **8c**, **9c** and **10a-c** at r_b =0.03 measured in 0.01 M (left) or 0.1 M (right) $NaClO_4$ plus 1 mM Tris/Cl with 0.1 mM EDTA, pH 7.4. ΔT_m is defined as the difference between the T_m values of platinated and nonmodified DNA. Data represent a mean ± SEM from two independent experiments.

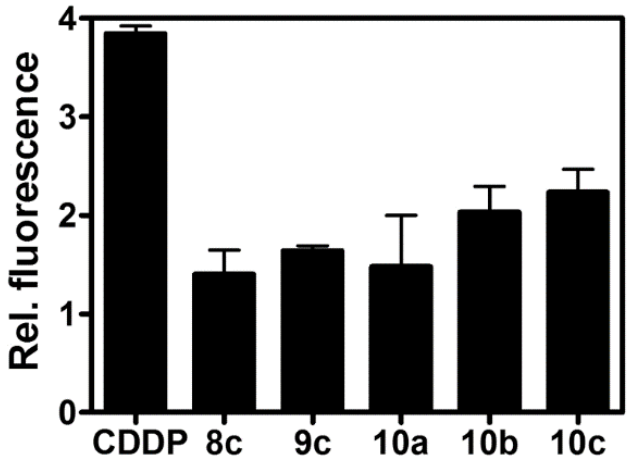

Fig. S 42. Changes in the relative fluorescence of Tb^{3+} ion bound to double-helical ctDNA modified by Pt complexes at $r_b = 0.03$. Tb^{3+} ion fluorescence of untreated DNA was arbitrarily set at 1. Values shown in the graph are the means (± SEM) of at least two independent measurements.

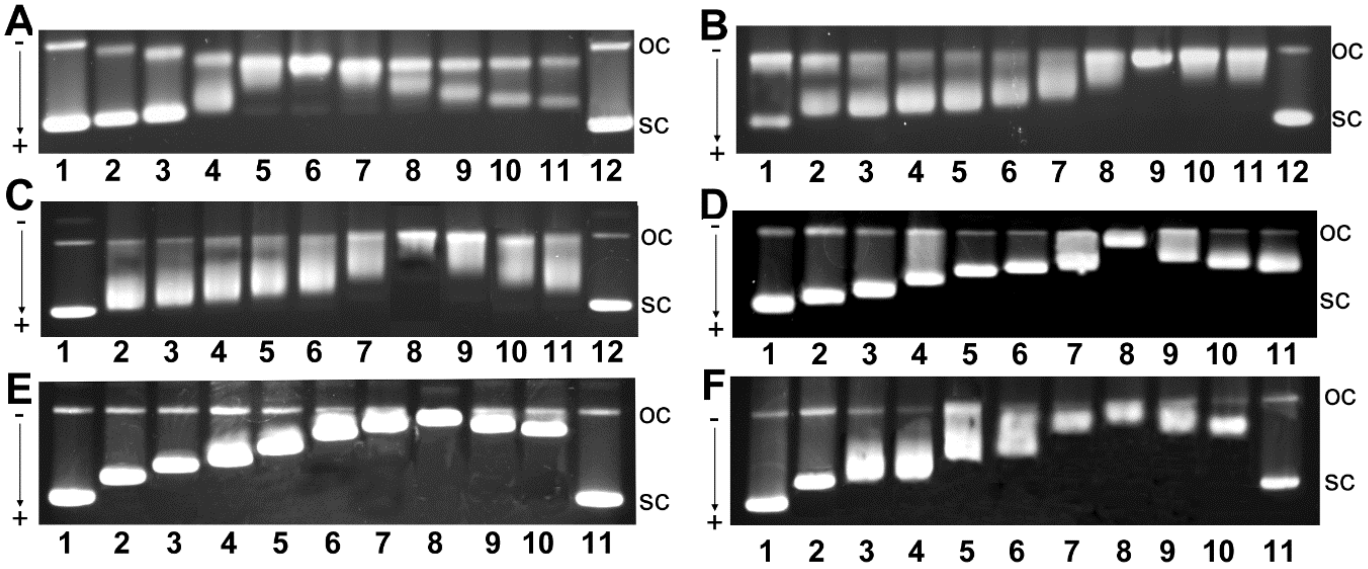

Fig. S 43. Unwinding of supercoiled pSP73 plasmid DNA by CDDP (A), **8c** (B), **9c** (C), **10a** (D, **10b** (E) and **10c** (F). The top bands correspond to the form of nicked plasmid (oc) and the bottom bands to the closed, negatively supercoiled plasmid (sc). A) lanes: 1 and 12, control, nonplatinated DNA; 2, r_b= 0.005; 3, r_b= 0.01; 4, r_b= 0.02; 5, r_b= 0.03; 6, r_b= 0.04; 7, r_b= 0.05; 8, r_b= 0.06; 9, r_b= 0.07; 10, r_b= 0.08; 11, r_b= 0.09. B) lanes: 1 and 12, control, nonplatinated DNA; 2, r_b= 0.03; 3, r_b= 0.04; 4, r_b= 0.05; 5, r_b= 0.056; 6, r_b= 0.06; 7, r_b= 0.07; 8, r_b= 0.077; 9, r_b= 0.084; 10, r_b= 0.09; 11, r_b= 0.1. C) lanes: 1 and 12, control, nonplatinated DNA; 2, r_b= 0.055; 3, r_b= 0.06; 4, r_b= 0.064; 5, r_b= 0.07; 6, r_b= 0.073; 7, r_b= 0.078; 8, r_b= 0.085; 9, r_b= 0.09; 10, r_b= 0.096; 11, r_b= 0.1. D) lanes: 1 and 12, control, nonplatinated DNA; 2, r_b= 0.052; 3, r_b= 0.06; 4, r_b= 0.07; 5, r_b= 0.074; 6, r_b= 0.08; 7, r_b= 0.085; 8, r_b= 0.093; 9, r_b= 0.1; 10, r_b= 0.11; 11, r_b= 0.12. E) lanes: 1 and 12, control, nonplatinated DNA; 2, r_b= 0.04; 3, r_b= 0.05; 4, r_b= 0.058; 5, r_b= 0.065; 6, r_b= 0.075; 7, r_b= 0.08; 8, r_b= 0.087; 9, r_b= 0.091; 10, r_b= 0.1; 11, r_b= 0.11. F) lanes: 1 and 12, control, nonplatinated DNA; 2, r_b= 0.045; 3, r_b= 0.052; 4, r_b= 0.054; 5, r_b= 0.06; 6, r_b= 0.065; 7, r_b= 0.07; 8, r_b= 0.079; 9, r_b= 0.085; 10, r_b= 0.1; 11, r_b= 0.11.

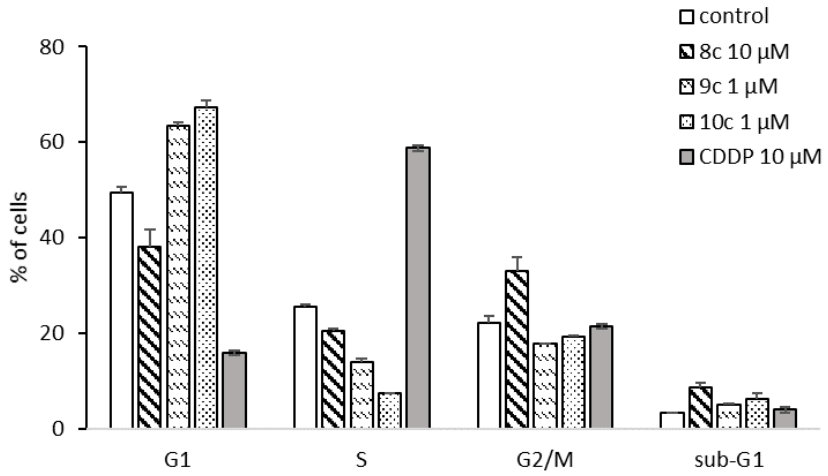

Fig. S 44: Effects of **8c** (10 µM), **9c** (1 µM), **10c** (1 µM), **CDDP** (10 µM) on the progression of the cell cycle of HCT116 $p53^{-/-}$ colon carcinoma cells after 24 h of treatment in comparison to untreated cells (vehicle control). The bars represent the percentages of cells in each phase of the cell cycle (G1, S and G2/M) and dead cells (sub-G1). Analysis was done via propidium iodide staining and flow cytometry, values represent means ± SDs of three experiments.

References

[1] R. Rubbiani, I. Ott *et al.*, *J. Med. Chem.*, 2010, **53**, 8608–8618, DOI: 10.1021/jm100801e.

[2] H. Valdés, M. Poyatos, G. Ujaque, E. Peris, *Chem. Eur. J.*, 2015, **21**, 1578 – 1588, DOI: 10.1002/chem.201404618.

[3] H. Lu and R. L. Brutchey, *Chem. Mater.,* 2017, **29**, 1396−1403, DOI: 10.1021/acs.chemmater.6b05293.